

# $\bar{d} - \bar{u}$ asymmetry and semi-inclusive production of pions in DIS

A. Szczurek<sup>1</sup>, V. Uleshchenko<sup>1,2</sup> and J. Speth<sup>3</sup>

<sup>1</sup> *Institute of Nuclear Physics, PL-31-342 Cracow, Poland*

<sup>2</sup> *Institute for Nuclear Research, 03-028 Kiev, Ukraine*

<sup>3</sup> *Institut für Kernphysik, KFA, Jülich, Germany*

November 5, 2018

## Abstract

We investigate unambiguities in the extraction of the  $\bar{d} - \bar{u}$  asymmetry from semi-inclusive production of pions in DIS. The role of several effects beyond the quark-parton model (QPM) which lead to  $N_p^{\pi^+} \neq N_n^{\pi^+}$  and  $N_p^{\pi^-} \neq N_n^{\pi^-}$  and may therefore cloud such an extraction is studied. The results are discussed in the context of the recent HERMES data. We find that the interaction of the resolved photon with the nucleon significantly modifies the observed  $\bar{d} - \bar{u}$  asymmetry. The exclusive elastic production of  $\rho$  mesons plays a similar role for the large- $z$  data sample. Our estimate shows a rather small effect of the spectator mechanism. Nuclear effects in the deuteron also look potentially important but are difficult to estimate quantitatively.

Throughout the paper we make in addition several general remarks concerning semi-inclusive and exclusive production of mesons.

## 1 Introduction

Since the NMC publication [1] on the Gottfried Sum Rule violation the effect of  $\bar{d} - \bar{u}$  asymmetry was in the 90's one of the most intensively discussed problems of nucleon structure. The effect is clearly of nonperturbative nature and was qualitatively explained as due to the pion (meson) cloud in the nucleon (for recent reviews see [2]). In order to shed more light on the nature of the Gottfried Sum Rule violation two different Drell-Yan experiments

were proposed and performed [3, 4]. They measured the ratio  $\sigma_{pd}^{DY}/\sigma_{pp}^{DY}$ . The integrated result for the asymmetry from the more complete Fermilab experiment [4] is  $\int_0^1[\bar{d} - \bar{u}] dx = 0.09 \pm 0.02$ , to be compared with the NMC result:  $\int_0^1[\bar{d} - \bar{u}] dx = 0.148 \pm 0.039$ . The NMC asymmetry appears slightly bigger. It was suggested recently by two of us that the difference can be partly due to large higher-twist effects for the nonsinglet quantity  $F_2^p - F_2^n$  [5].

It was proposed in Ref.[6] how to use semi-inclusive production of pions to extract the asymmetry of light antiquarks in the nucleon. This method was applied recently by the HERMES collaboration at HERA [7].

Recent results for semi-inclusive production of pions in polarized photo-production obtained at SLAC [8] have shown that spin asymmetry almost cancels for small transverse momenta of the outgoing pions, which seems to be another nonperturbative effect. This result was interpreted as a large VDM contribution [9] for small transverse momenta. Only at large transverse momenta may the perturbative QCD processes reveal themselves and only then can one try to disentangle the polarized quark distributions in the nucleon. At low photon virtuality, as in the HERMES experiment where  $\langle Q^2 \rangle \sim 2.3 \text{ GeV}^2$ , similar nonperturbative effects can be expected in the unpolarized case.

In the present paper we try to examine the semi-inclusive production of pions in DIS as a source for measuring the  $\bar{d} - \bar{u}$  asymmetry. We investigate several effects, mostly of nonperturbative nature, which may modify the resulting asymmetry. In particular, making quantitative estimations, we focus on conclusions relevant for the HERMES experiment.

## 2 Quark-parton model approach

### 2.1 Extraction of the $\bar{d} - \bar{u}$ asymmetry

The most general five-fold cross section for one-particle semi-inclusive unpolarized lepton-hadron scattering can be expressed in terms of four independent semi-inclusive structure functions (see for instance [10]). If the azimuthal correlation between the lepton scattering plane and the hadron production plane is not studied, the number of independent structure func-

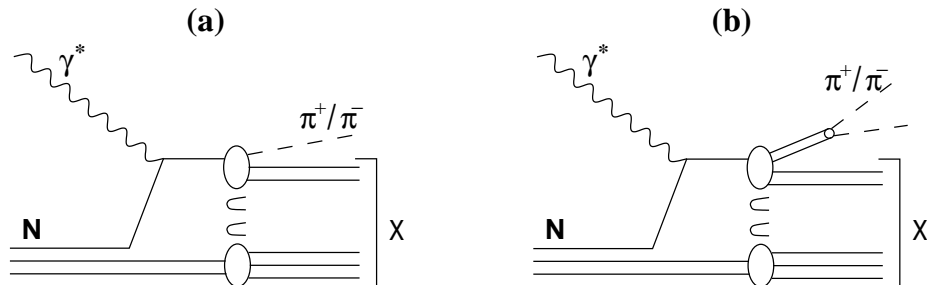


Figure 1: *Partonic mechanisms of pion production: (a) direct fragmentation of quark into a pion (b) fragmentation of quark into an intermediate hadronic resonance and its subsequent decay.*

tions reduces to two. Then the cross section can be written as

$$\frac{d\sigma}{dx dQ^2 dz dp_{h,\perp}^2} = \frac{4\pi\alpha^2}{Q^4 x} [y^2 2x \mathcal{F}_1(x, Q^2, z, p_{h,\perp}^2) + 2(1-y) \mathcal{F}_2(x, Q^2, z, p_{h,\perp}^2)], \quad (1)$$

where  $x$ ,  $y$  and  $Q^2$  are standard DIS variables,  $p_{h,\perp}$  is the transverse momentum of the detected hadron with respect to the momentum of the virtual photon and

$$z = \frac{P \cdot p_h}{P \cdot q} \stackrel{TRF}{=} \frac{E_h}{\nu} \quad (2)$$

is a relativistically invariant variable which in the target rest frame is the fraction of the virtual photon energy  $\nu$  carried by the hadron. In the formula above,  $P$ ,  $p_h$  and  $q$  are the four-momenta of the target nucleon, final hadron and virtual photon, respectively.

If one is not interested in the transverse momentum distribution of the emitted hadron then the triple-differential cross section can be written in a more compact way

$$\frac{d\sigma}{dx dQ^2 dz} = \frac{4\pi\alpha^2}{Q^4 x} [y^2 2x \mathcal{F}_1(x, Q^2, z) + 2(1-y) \mathcal{F}_2(x, Q^2, z)]. \quad (3)$$

In the quark-parton model (QPM) only mechanisms shown in Fig.1 are assumed. Usually in calculations one does not distinguish diagrams (a) and (b). It is commonly believed that diagram (b) can be included effectively on

the same footing as diagram (a). We shall discuss later possible restrictions of such an approach.

In the naive QPM the generalized semi-inclusive structure functions  $\mathcal{F}_1$  and  $\mathcal{F}_2$  are related by the Callan-Gross relation leaving only one independent structure function, which can be written as

$$\mathcal{F}_2^{N \rightarrow \pi}(x, Q^2, z) = \sum_f e_f^2 x q_f(x, Q^2) \cdot D_{f \rightarrow \pi}(z), \quad (4)$$

where the sum runs over the quark/antiquark flavours  $f = u, d, s$ ;  $q_f$  are quark distribution functions and  $D_{f \rightarrow \pi}(z)$  are so-called fragmentation functions [11].

Quite a number of fragmentation functions can be reduced by the requirement of isospin symmetry and charge conjugation:

$$\begin{aligned} D_u^{\pi^+}(z) &= D_d^{\pi^+}(z) = D_d^{\pi^-}(z) = D_u^{\pi^-}(z) \\ &\equiv D_+(z) \end{aligned} \quad (5)$$

for the favoured fragmentation and

$$\begin{aligned} D_d^{\pi^+}(z) &= D_u^{\pi^+}(z) = D_u^{\pi^-}(z) = D_d^{\pi^-}(z) \\ &\equiv D_-(z) \end{aligned} \quad (6)$$

for the unfavoured fragmentation. For the strange/antistrange fragmentation, in principle, a third type of fragmentation functions has to be assumed. In the following we shall assume simply:

$$D_s^{\pi^+}(z) = D_{\bar{s}}^{\pi^+}(z) = D_s^{\pi^-}(z) = D_{\bar{s}}^{\pi^-}(z) = S_{red} \cdot D_-(z), \quad (7)$$

where  $S_{red}$  is a reduction factor with respect to nonstrange quarks/antiquarks. In calculations we shall use  $S_{red} = 1.0$ .<sup>1</sup>

Now, in the quark-parton model (4) using symmetry relations (5-6) one can combine semi-inclusive cross sections for the production of positive and negative pions on proton and neutron targets and isolate a quantity sensitive to the flavour asymmetry [7]

$$\frac{\bar{d}(x) - \bar{u}(x)}{u(x) - d(x)} = \frac{J(z)[1 - r(x, z)] - [1 + r(x, z)]}{J(z)[1 - r(x, z)] + [1 + r(x, z)]}, \quad (8)$$

---

<sup>1</sup>This appears to be not very important in practice.

where  $J(z) = \frac{3}{5} \frac{1+D_-(z)/D_+(z)}{1-D_-(z)/D_+(z)}$  and  $r(x, z) = \frac{N_p^{\pi^-}(x, z) - N_n^{\pi^-}(x, z)}{N_p^{\pi^+}(x, z) - N_n^{\pi^+}(x, z)}$  is a ratio of differences of charged pion yields on proton and neutron. It is straightforward to see that the fragmentation of strange quarks/antiquarks cancels in the quantity  $r(x, z)$ . It is also worth noting that the r.h.s. in Eq.(8), formally dependent on  $z$ , gives a quantity independent of  $z$ .

Thus semi-inclusive production of charged pions in DIS allows us to determine the asymmetry of light sea quarks. Although this is on condition that the QPM works well, that is, one may neglect the influence of other possible mechanisms.

## 2.2 Intermediate resonances in the fragmentation

It is a well known fact that pions produced directly in the fragmentation process constitute only a fraction of all pions registered in detectors. The contribution of pions coming from the decay of heavier mesons is of the same order of magnitude [12, 13, 14].

Because the intermediate resonances originate from the fragmentation of the struck quark their contribution can be included into an overall “effective” fragmentation function. Modern analyses of fragmentation functions do not treat intermediate resonances explicitly, just include them effectively by fitting total inclusive data. However, it is not clear, a priori, whether under a more detailed consideration such an effective treatment is correct and whether resonances do not disturb the identity (8).

To treat the intermediate resonances explicitly we write down the fragmentation function as a sum of two parts: a direct fragmentation component (Fig.1a) and a resonance component (Fig.1b):

$$D_{f \rightarrow \pi} = \tilde{D}_{f \rightarrow \pi} + \sum_R D_{f \rightarrow R \rightarrow \pi}, \quad (9)$$

where  $\tilde{D}_{f \rightarrow \pi}$  is a fragmentation function of the direct fragmentation of a quark  $f$  into a pion  $\pi$ ,  $D_{f \rightarrow R \rightarrow \pi}$  describes the production of a pion  $\pi$  through an intermediate resonance  $R$  and the sum runs over all possible resonances. It is known experimentally that for pion production the vector meson intermediate states are the most important. For not too small  $z$ , neglecting for simplicity transverse momenta, the contribution of the resonance  $R$  to the fragmentation function can be approximated as

$$D_{f \rightarrow R \rightarrow \pi}(z) = \int_{z_0}^1 \tilde{D}_{f \rightarrow R}(z') \cdot f_{R \rightarrow \pi}\left(\frac{z}{z'}\right) dz, \quad (10)$$

where  $z_0 = \max(z, z_{min}^R)$ ,  $z_{min}^R$  is the minimal possible  $z$  of the resonance  $R$ ,  $\tilde{D}_{f \rightarrow R}$  is a fragmentation function for the direct fragmentation of a quark  $f$  into a resonance  $R$ , and  $f_{R \rightarrow \pi}$  describes the decay of the resonance  $R$  to pionic channels.

The fragmentation process transforms quarks with the third component of isospin  $I_3^q = \pm \frac{1}{2} \Leftrightarrow \begin{Bmatrix} u & \bar{d} \\ d & \bar{u} \end{Bmatrix}$  into measured pions with  $I_3^\pi = \pm 1 \Leftrightarrow \begin{Bmatrix} \pi^+ \\ \pi^- \end{Bmatrix}$  i.e. there are two initial and two final states of fragmentation with respect to  $I_3$ . If the quark hadronization is driven by the strong interaction (isospin symmetric) then, in the case of direct fragmentation, one naturally obtains only two kinds of fragmentation functions related by (5-6). For the resonance contribution  $D_{f \rightarrow \pi}^R \equiv \sum_R D_{f \rightarrow R} f_{R \rightarrow \pi}$ , if the sum comprises all possible intermediate states and if in addition the isospin is conserved in the decay of resonances, one still has only two kinds of fragmentation functions:

$$D_+^R \equiv \sum_R D \begin{Bmatrix} u & \bar{d} \\ d & \bar{u} \end{Bmatrix} \rightarrow R \rightarrow \begin{Bmatrix} \pi^+ \\ \pi^- \end{Bmatrix} \quad (11)$$

and

$$D_-^R \equiv \sum_R D \begin{Bmatrix} u & \bar{d} \\ d & \bar{u} \end{Bmatrix} \rightarrow R \rightarrow \begin{Bmatrix} \pi^- \\ \pi^+ \end{Bmatrix} . \quad (12)$$

These functions correspond uniquely to the standard favoured and unfavoured fragmentation functions and fulfil the relation (5-6) needed to obtain the identity (8). Thus we come to the conclusion that intermediate resonances do not violate Eq.(8) i.e. do not disturb the procedure of extraction of the  $\bar{d} - \bar{u}$  asymmetry.

However, one cannot avoid completely the explicit treatment of intermediate resonances when modelling pion spectra. The fragmentation functions (9) with the resonance components (10) do not (!) obey the QCD evolution equation; this is usually ignored in the current literature. It would be useful to separate out the direct fragmentation contribution to the fragmentation functions, which has a better chance of obeying the QCD evolution equations. However, to determine the fragmentation functions of the direct fragmentation one would need to perform a combined analysis of fragmentation into pions and into all other resonances having pionic decay channels. Such an involved experimental analysis has never yet been done.

### 2.3 Choice of fragmentation functions

In order to estimate the effect of nonpartonic components on the extraction of  $\bar{d} - \bar{u}$  asymmetry we need to fix fragmentation functions with which the main partonic term will be calculated.

Modern parametrizations of fragmentation functions are fitted mostly to data from  $e^+e^-$  collisions. These analyses include leading or next-to-leading order QCD corrections (see for instance [15, 16, 17]). In contrast to  $e^+e^-$  collisions the situation in  $ep$  scattering is much less developed: less experimental data, no QCD analysis.

Let us see how the existing parametrizations of fragmentation functions behave in  $ep$  collisions. We start the quantitative estimations by comparing the existing fragmentation functions with the  $z$ -distributions of charged pions in  $ep$  scattering. In Fig.2 we present  $\frac{1}{\sigma}(\frac{d\sigma^{\pi^+}}{dz} + \frac{d\sigma^{\pi^-}}{dz})$  data obtained long

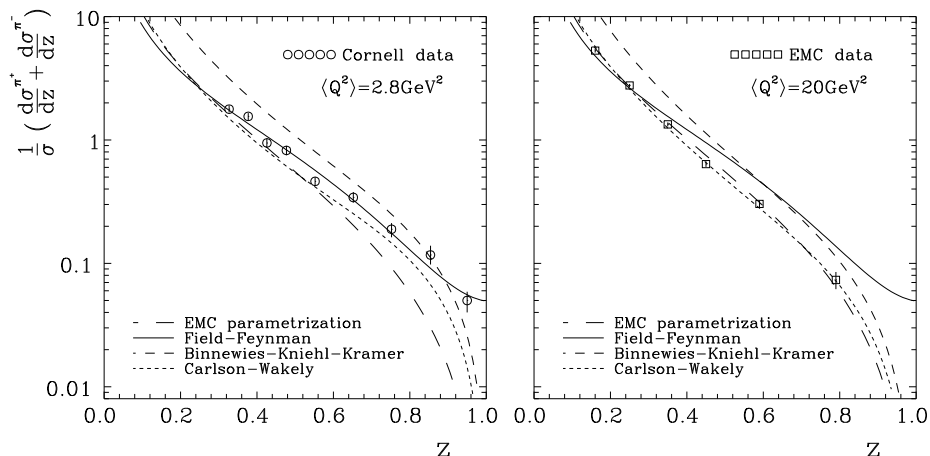


Figure 2: Multiplicity distribution of charged pions  $\frac{1}{\sigma}(\frac{d\sigma^{\pi^+}}{dz} + \frac{d\sigma^{\pi^-}}{dz})$  in DIS. Different sets of fragmentation functions are confronted with the Cornell [18] data with  $2 < Q^2 < 6 \text{ GeV}^2$  and  $W \sim 3\text{-}4 \text{ GeV}$  (left panel) and the EMC [19] data with  $20 < \langle Q^2 \rangle < 71 \text{ GeV}^2$ , depending on  $z$  (right panel).

ago at Cornell [18] (panel a) with kinematics similar to the HERMES experiment, and the data from EMC [19] (panel b) with slightly higher  $Q^2$ . We show also the QPM predictions obtained with fragmentation functions from the fit to  $e^+e^-$  data [16], from the fit to  $e^+e^-$  and photoproduction data [20] which include QCD corrections, and with fragmentation functions from the simple QPM fits to the  $ep$  data [21, 19]. Surprisingly the “advanced”

parametrizations give a much worse description of the data than simple ones do. However, simple parametrizations are limited to the relevant values of  $Q^2$ .

In principle the modern fragmentation functions used in  $e^+e^-$  [16] were obtained including QCD corrections, i.e. beyond the naive quark-parton model. The correct formulae for the cross section in DIS calculated including QCD corrections are more complicated than QPM ones [23, 24]. On the other hand the analysis of the HERMES experiment [7] was performed based on simple QPM formulae, using Eq.(8). Therefore in order to compare with those results we have to stay at the QPM level too and ignore some inconsistency. Moreover the QCD evolution of fragmentation functions (included in the calculation) changes the pion multiplicity in agreement with the trend of experimental data and might create the main part of the  $Q^2$ -dependence even when used with QPM formulae. The whole effect of the inconsistency should, however, be clarified in the future.

In electron-positron scattering the number of negative and positive pions produced is identical. This is not the case for  $ep$  scattering. Here quark distributions in the proton, isospin-asymmetric by their nature, allow us to distinguish between the favoured and unfavoured fragmentation which is very difficult, if not impossible, in  $e^+e^-$  scattering. As can be seen from Eq.(8) such a separation is essential for our analysis. In Fig.3 we show  $z$ -distributions of negative (upper panel) and positive (lower panel) pions as measured by the EMC collaboration [19]. Different sets of fragmentation functions are confronted with the experimental data. A surprisingly poor description of the data is obtained with fragmentation functions from  $e^+e^-$  scattering [16]. Not very good agreement of the Field-Feynman parametrization is most probably due to a different  $Q^2$  here ( $\sim 20 \text{ GeV}^2$ ) than that where it was designed [21]. A correct QCD evolution should resolve this disagreement. As will be discussed below both QPM-parametrizations give reasonable representations of the ratio of unfavoured to favoured fragmentation functions, which is a more slowly QCD-evolving quantity.

The ratio  $D_-(z)/D_+(z)$  directly enters formula (8) and, as our analysis shows, the measured  $\bar{d} - \bar{u}$  asymmetry is very sensitive to it. In Fig.4 we display the ratio obtained from the analysis of experimental data from EMC [33] and recently obtained by the HERMES collaboration at DESY [34]. The simple QPM parametrizations [21, 19] provide a reasonable description of the data. In contrast the “advanced” fragmentation functions [16, 20] fail again. Is it due to a different physics in  $e^+e^-$  collisions than in DIS, or is it due to QCD corrections, or is it due to something else? In our opinion this



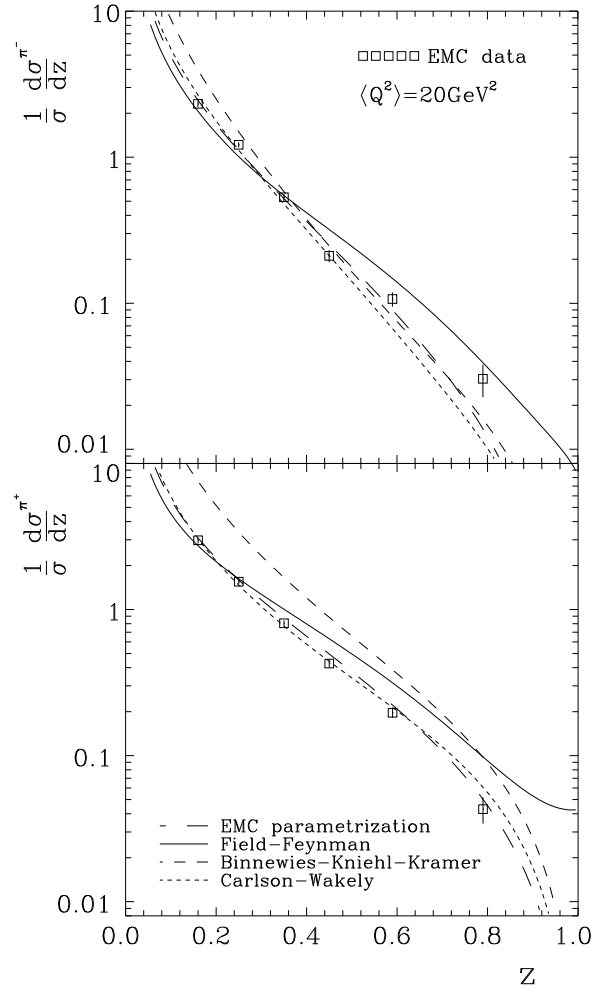


Figure 3:  $\frac{1}{\sigma} \left( \frac{d\sigma_{\pi^-}}{dz} \right)$  (upper panel) and  $\frac{1}{\sigma} \left( \frac{d\sigma_{\pi^+}}{dz} \right)$  (lower panel). The experimental data are taken from [19]. The fragmentation functions used are the same as in the previous figure.

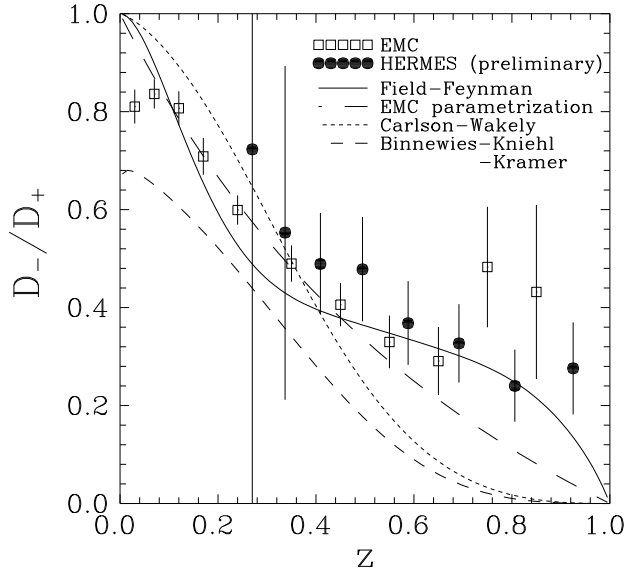


Figure 4: *The ratio of unfavoured to favoured fragmentation functions as a function of  $z$ . The experimental data are from EMC [33] and from a preliminary, unpublished HERMES analysis [34].*

is mainly due to the fact that the  $e^+e^-$  data are not sufficient to separate unambiguously the favoured and unfavoured fragmentation functions. A QCD analysis of DIS fragmentation functions is called for.

The analysis above advocates the Field-Feynman parametrization [21] as the only good representation of the available  $ep$  data in the HERMES kinematical region. This parametrization will be used in the following analysis.

### 3 Nonpartonic components

For small  $Q^2$ , as for the HERMES experiment, some mechanisms of nonpartonic origin (see e.g. Fig.5) may become important. For instance, the virtual photon can interact with the nucleon via its intermediate hadronic state. Such a mechanism is usually described within the vector dominance model (VDM). The photon could also fluctuate into a pair of pions, where both or one of them interact with the nucleon. In addition some exclusive

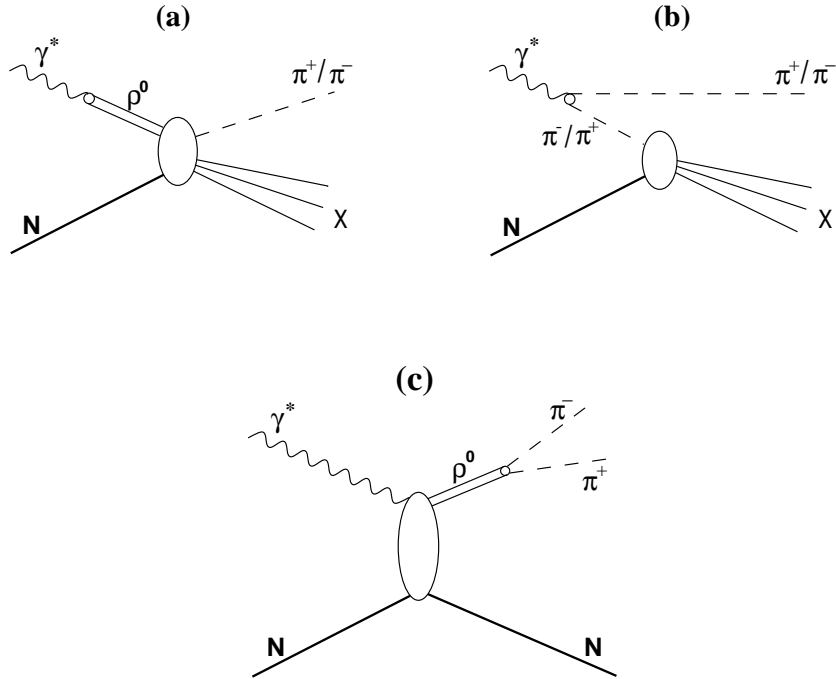


Figure 5: *Nonpartonic mechanisms of pion production taken into account in this work: (a) VDM contribution, (b) spectator mechanism, (c) elastic production of the  $\rho^0$  meson and its decay.*

processes can produce pions directly or as decay products of heavier mesons.

To our best knowledge none of such processes has been investigated in the literature. Their influence on the extracted  $\bar{d}-\bar{u}$  asymmetry also remains unknown. We shall discuss processes shown in Fig.5 one by one.

### 3.1 Central VDM contribution

Let us start from the VDM component (see Fig.5a). It was shown that in the inclusive DIS incorporation of the VDM contribution and related modification of the partonic component help to understand the behaviour of structure functions  $F_2^p$  and  $F_2^d$  at small  $Q^2$  [31, 32]. This model was confirmed by a recent analysis of the  $Q^2$  dependence of the world data for the structure function difference  $F_2^p - F_2^n$  [5].

The model for inclusive structure functions [31, 32] can be generalized to semi-inclusive production of pions:

$$\begin{aligned} \mathcal{F}_2^{N \rightarrow \pi}(x, Q^2, z) &= \frac{Q^2}{Q^2 + Q_0^2} \sum_f e_f^2 x q_f(x, Q^2) \cdot D_{f \rightarrow \pi}(z) \\ &+ \frac{Q^2}{\pi} \sum_V \frac{1}{\gamma_V^2} \frac{\sigma_{VN \rightarrow \pi X}(s^{1/2}) M_V^4}{(Q^2 + M_V^2)^2} \Omega_V(x, Q^2). \end{aligned} \quad (13)$$

The second sum above runs over vector mesons  $V = \rho^0, \omega, \phi$  and  $\Omega_V$  is a correction factor which takes into account finite fluctuation times of the virtual photon into vector mesons for large  $x$  [32].

The inclusive cross section for pion production in vector meson ( $\rho^0, \omega, \phi$ ) scattering off the proton and neutron is not known experimentally. There is no model in the literature that one can trust quantitatively but in analogy to the total  $\rho^0 N$  cross section the cross section  $\rho^0 N \rightarrow \pi^\pm X$  can be estimated as:

$$\begin{aligned} \sigma(\rho^0 p \rightarrow \pi^\pm X) &\approx 1/2 [\sigma(\pi^+ p \rightarrow \pi^\pm X) + \sigma(\pi^- p \rightarrow \pi^\pm X)] \\ \sigma(\rho^0 n \rightarrow \pi^\pm X) &\approx 1/2 [\sigma(\pi^+ n \rightarrow \pi^\pm X) + \sigma(\pi^- n \rightarrow \pi^\pm X)]. \end{aligned} \quad (14)$$

Experimental data from the ABBCCHW collaboration [36] at  $p_{lab}^\pi = 8, 16$  GeV correspond approximately to the range of the HERMES experiment [7]. Unfortunately as it often happens in high-energy physics there is only data for proton targets. Using isospin symmetry for hadronic reactions one can obtain corresponding cross sections on the neutron from those on the proton by assuming

$$\sigma(\rho^0 n \rightarrow \pi^+ X) = \sigma(\rho^0 p \rightarrow \pi^- X), \quad (15)$$

$$\sigma(\rho^0 n \rightarrow \pi^- X) = \sigma(\rho^0 p \rightarrow \pi^+ X). \quad (16)$$

These relations hold not only for the total cross sections but also for differential ones independently of energy. From the most complete data at  $p_{lab}^\pi = 16$  GeV [36] ( $W = 5.56$  GeV) we get

$$1/2 [\sigma(\pi^+ p \rightarrow \pi^+ X) + \sigma(\pi^- p \rightarrow \pi^+ X)] = 38.65 \pm 0.29 \text{ mb},$$

$$1/2 [\sigma(\pi^+ p \rightarrow \pi^- X) + \sigma(\pi^- p \rightarrow \pi^- X)] = 31.80 \pm 0.22 \text{ mb};$$

clearly different values. Although the bulk of the difference comes from the target fragmentation region, which we are not interested in, in the beam fragmentation region it was also found  $\sigma(\pi^+ p \rightarrow \pi^- X) = 14.8$  mb and

$\sigma(\pi^- p \rightarrow \pi^+ X) = 19.0$  mb [36] with almost equal cross sections for beam-like pions.

The situation in the semi-inclusive case is more complicated than for total cross sections. The experimental spectra for  $\pi^\pm p \rightarrow \pi^\pm X$  contain components due to peripheral processes, which are, in general, specific, different for different reactions. Peripheral processes from the  $\pi^+ p \rightarrow \pi^+ X$  and  $\pi^- p \rightarrow \pi^- X$  reactions do not contribute to the  $\rho^0 p \rightarrow \pi^\pm X$  reaction and should be eliminated; only nondiffractive components of the  $\pi p \rightarrow \pi X$  reactions should be taken into account when modelling  $\rho^0$ -induced reactions.<sup>2</sup> This requires physically motivated parametrization of the  $\pi N \rightarrow \pi X$  data.

Following these arguments we have parametrized the experimental differential cross sections for four different reactions  $\pi^\pm p \rightarrow \pi^\pm X$  from [36] as a sum of central and peripheral components

$$\frac{d\sigma}{dx_F dp_\perp^2} = \frac{d\sigma^{cen}}{dx_F dp_\perp^2} + \frac{d\sigma^{per}}{dx_F dp_\perp^2}, \quad (17)$$

where  $x_F$  is the well known Feynman variable. Details of this analysis will be presented elsewhere, a short sketch is given in Appendix A. Because the CM-energy of the ABBCCHW collaboration is very similar to that of the HERMES experiment, we believe that in the range of energy relevant for this experiment the functional form given in the appendix is suitable.

Finally, our analysis of experimental data [36] combined with the assumption of isospin symmetry (16) shows that for the nondiffractive components still

$$\sigma(\rho^0 p \rightarrow \pi^\pm X) \neq \sigma(\rho^0 n \rightarrow \pi^\pm X). \quad (18)$$

In Fig.6 we show

$$\delta_{pn}^{\rho^0 \rightarrow \pi^\pm} = \frac{\sigma(\rho^0 p \rightarrow \pi^\pm X) - \sigma(\rho^0 n \rightarrow \pi^\pm X)}{\sigma(\rho^0 p \rightarrow \pi^\pm X) + \sigma(\rho^0 n \rightarrow \pi^\pm X)} \quad (19)$$

for both positive and negative pions. An identical value of the asymmetry is expected for the  $\omega$  beam and a similar one for the  $\phi$  beam. This automatically means practically the same result for photon (real or virtual) induced reactions which proceed via hadronic intermediate states. We obtain rather large asymmetries, larger than for total photoproduction cross sections on the proton and neutron.

---

<sup>2</sup> Some peripheral processes specific for the  $\rho^0$  beam will be included explicitly in section 3.3.

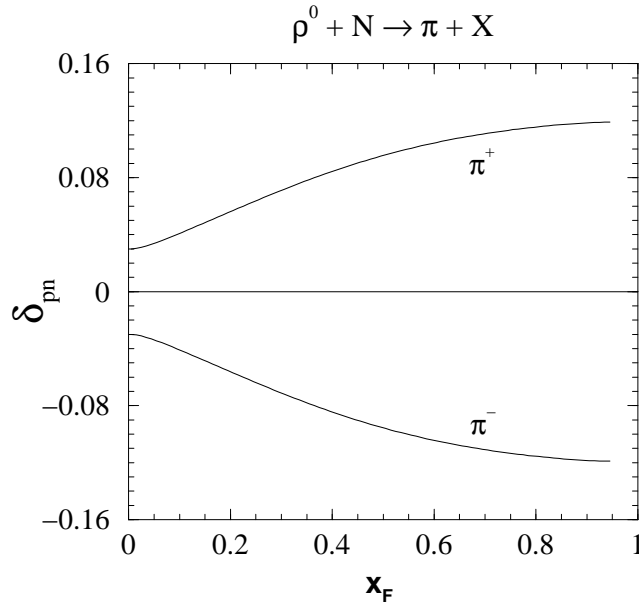


Figure 6:  $\delta_{pn}^{\rho^0 \rightarrow \pi^\pm}$  calculated from Eq.(19) as a function of Feynman  $x_F$ . The pion+proton cross sections were taken from the parametrization described in Appendix A.

Different cross sections on proton and neutron mean that the VDM contribution modifies the r.h.s. of Eq.(8). In Fig.7 we show a modification of the measured quantity  $\frac{\bar{d}-\bar{u}}{u-d}$  due to the central VDM component. In the HERMES experiment [7] both  $Q^2$  and  $W$  vary with Bjorken- $x$ , but the change of energy is considerably smaller. In the present calculation the photon-proton CM energy was fixed at the average HERMES value  $W = 5.0 \text{ GeV}^2$ . In the panel (a) we show a result of a calculation where the central VDM component discussed in this section is simply added to the main fragmentation component. In the panel (b) the fragmentation component in addition was rescaled by the factor  $\frac{Q^2}{Q^2+Q_0^2}$  (see Eq.(13)) which is required for consistency of inclusive and semi-inclusive structure functions. The solid line in both panels represents  $\frac{\bar{d}-\bar{u}}{u-d}$  obtained directly from the parton distributions [64]. As can be seen from the figure the r.h.s. of Eq.(8) clearly deviates from the assumed partonic outcome. The effect is surprisingly large, especially for

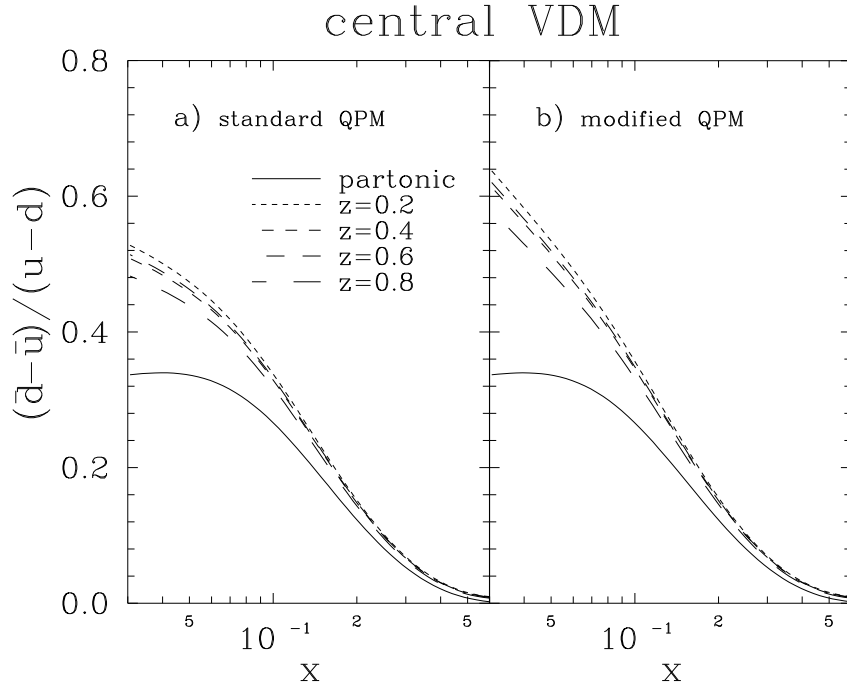


Figure 7: The true (solid) and the modified by the central VDM contribution  $\frac{\bar{d}-\bar{u}}{u-d}$ , calculated according to the l.h.s. and r.h.s. of Eq.(8), respectively, as a function of Bjorken- $x$  for different values of  $z$  and typical HERMES  $W = 5$  GeV. The result in panel (a) is obtained by a simple addition of the fragmentation and the central VDM components ( $Q_0^2 = 0$  in Eq.(13)). The result in panel (b) is obtained with the rescaled ( $Q_0^2 = 0.8$  GeV<sup>2</sup>) fragmentation component, as described in the text.

small  $x$ .<sup>3</sup> Thus, the quark flavour asymmetry extracted from semi-inclusive experiments in the simple QPM approach seems to be highly overestimated if the VDM contribution is neglected.

The VDM effect discussed in this section is not completely new. A similar effect of the hadronic structure of the photon on the difference of semi-inclusive cross sections  $\sigma_{\gamma p \rightarrow \pi^+ X} - \sigma_{\gamma p \rightarrow \pi^- X}$  was already noticed long ago in real photoproduction [42]. Although in DIS the effect is smaller, it, however, strongly modifies the measured  $\bar{d} - \bar{u}$  asymmetry.

### 3.2 Spectator mechanism

In both partonic and central VDM mechanisms the virtual photon is totally absorbed and pions are produced in a complex process involving many degrees of freedom. Such pions are then preferentially emitted at not very large values of  $z$ . The peripheral processes are not included either in the partonic or the central VDM component considered above and are expected to be important in the region of large  $z$  where these processes disappear. Let us consider first the spectator mechanism depicted in Fig.5b. To our knowledge such a mechanism has been never discussed in the literature for photon induced reactions. We begin with the case of real photoproduction where we can apply a technique from [37]. For virtual photons with  $q^2 < 0$  the formalism is not well developed.

The cross section for the spectator pions  $\pi^\pm$  in real photoproduction can be expressed as a product of the distribution of pions in the photon ( $f_{\pi^\pm/\gamma}$ ) and the off-shell total cross section for scattering of  $\pi^\pm$  off the proton or neutron:

$$\frac{d\sigma_{spect}^{\pi^\pm}}{dz} \approx f_{\pi^\pm/\gamma}(z) \cdot \sigma_{tot}^{\pi^\mp N}((1-z)s). \quad (20)$$

At small  $\pi N$  energies  $s_{\pi N} \approx (1-z)s_{\gamma^* N}$  relevant for the spectator mechanism there can be a difference between  $\sigma_{tot}^{\pi^+ p}$  and  $\sigma_{tot}^{\pi^- p}$ . Together with isospin symmetry of hadronic reactions this would lead to different  $N_p^{\pi^\pm}$  and  $N_n^{\pi^\pm}$  i.e. would modify the identity (8). To represent the total cross sections of  $\pi^\pm$  scattering off nucleons we use cubic interpolation of the world experimental data [38].

---

<sup>3</sup> We wish to remind the reader here that in the HERMES experiment the photon virtuality for small  $x$  is only of the order of 1 - 2 GeV<sup>2</sup>.



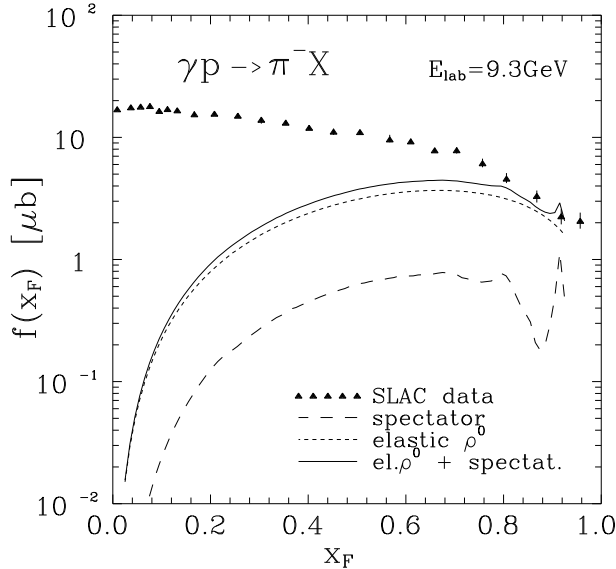


Figure 8: *The invariant structure function  $f(x_F)$  for the  $\gamma p \rightarrow \pi^- X$  reaction and  $E_\gamma = 9.3$  GeV.*

The distribution function  $f_{\pi^\pm/\gamma}$  can be calculated using a technique similar to that outlined in [37]:

$$f_{\pi^\pm/\gamma}(z, k_\perp^2) = \frac{g_{em}^2}{64\pi^2} \cdot \frac{1}{z(1-z)} \cdot \frac{2k_\perp^2}{[0 - M_{\pi\pi}^2(z, k_\perp^2)]^2} |F(z, k_\perp^2)|^2, \quad (21)$$

where  $g_{em}$  is the electromagnetic  $\gamma \rightarrow \pi^+\pi^-$  coupling constant,  $M_{\pi\pi}$  is the invariant mass of the two-pion system,  $F(z, k_\perp^2)$  is a vertex form factor which accounts for the finite size of particles involved and off-shell effects. For other technical details see [37].

In Fig.8 we show the result of our calculation (dashed line) with cut-off mass 1.5 GeV as in Ref.[37] for  $s^{1/2} = 4.28$  GeV corresponding to the experimental data from SLAC [39] with  $E_\gamma = 9.3$  GeV. The results are presented in terms of the invariant single particle structure function [39] (see also Eq.(43) in Appendix A). The energy in the pion-proton subsystem decreases with increasing  $x_F$  and we observe fluctuations due to  $s$ -channel  $\pi N$  resonances. The peaks would be even more pronounced at smaller photon energies and would disappear completely at larger photon energies.

The contribution of the spectator mechanism calculated with reasonable cut-off masses in the vertex form factor is smaller than experimental data. A dominant fraction of pions produced at large  $x_F$  appears to be given by the mechanism of elastic  $\rho^0$ -meson production and its subsequent decay (discussed in detail in section 3.3). By the short-dashed line we present this contribution corresponding to the cross section calculated as:

$$\frac{d\sigma^{\rho^0 \rightarrow \pi^\pm}}{dz} = \sigma(\gamma p \rightarrow \rho^0 p) \cdot f_{decay}^{\rho^0 \rightarrow \pi^\pm}(z), \quad (22)$$

where the explicit functional form of the decay function  $f_{decay}^{\rho^0 \rightarrow \pi^\pm}(z)$  can be found in Appendix B. In the calculation we have used the experimental value  $\sigma(\gamma p \rightarrow \rho^0 p) = 13 \mu\text{b}$ , relevant for  $E_\gamma = 9.3 \text{ GeV}$ . The sum of both contributions (solid line) seems to be consistent with the large- $x_F$  part of the pion spectrum. Thus in real photoproduction the spectator mechanism becomes non-negligible only at large  $x_F$  (or  $z$ ).

In virtual photoproduction the situation is more complicated. The absolute normalization of  $f_{\pi^\pm/\gamma^*}$  should depend on the virtuality of the photon. However, it cannot be calculated from first principles as it involves a vertex form factor where more than one particle is off mass shell. Empirically such cases are strongly damped [40]. Also a naive use of a typical light-cone parametrization of the vertex form factors [37] with the mass of the parent particle replaced by the virtuality of the photon leads to a strong suppression in comparison to real photoproduction. How strong this suppression is in comparison to the suppression of the elastic- $\rho^0$  production mechanism is not clear. For photon virtualities of the order of  $Q^2 \sim 2\text{-}4 \text{ GeV}^2$  we find that the elastic- $\rho^0$  contribution, discussed in detail in the next section, together with the partonic component, totally accounts for the cross sections at large  $z$ , leaving practically no room for the spectator mechanism (see Fig.16).

In summary, the spectator mechanism, while potentially important in real photoproduction is most probably negligible in DIS.

### 3.3 Exclusive $\rho$ meson production

The exclusive meson production  $\gamma^* N \rightarrow MN'$  is one more mechanism not included in the fragmentation formalism (Eq.(4)) and may also modify the extraction of the  $\bar{d} - \bar{u}$  asymmetry. The pion exclusive channels ( $M = \pi$ )<sup>4</sup>

---

<sup>4</sup> These are not included in the spectator mechanism discussed above where the final state  $X = N$  was not taken into account.

contribute at  $z \approx 1$ , i.e. outside of the range of the HERMES kinematics and will be ignored in the following discussion. In contrast, the pions from the decays of light vector mesons may be important in the context of the  $\bar{d} - \bar{u}$  asymmetry from semi-inclusive pion production. The production of  $\rho$  mesons ( $M = \rho$ ) seems to be of particular importance. Firstly, the  $\rho^0 N$  channel is known to be the dominant exclusive channel in  $\gamma^* N$  scattering. Secondly, because  $\rho^0$  decays predominantly into two pions this will produce pions with  $\langle z \rangle \sim \frac{1}{2}$ . A detailed calculation (see Appendix B) shows that the dispersion of the decay pion  $z$ -distribution is large and therefore this effect has a chance of being observed at large  $z$  where the hadronization rate is already much smaller. The next potentially important mechanism is the  $\omega$  meson ( $M = \omega$ ) production. However, the dominant  $\omega$  meson decay channel is the three-body system  $\pi^+ \pi^- \pi^0$  i.e. it is expected to contribute to the inclusive pion distribution at  $\langle z \rangle \sim \frac{1}{3}$ , i.e. in the region where the hadronization rate is large. Moreover the cross section for the  $\omega$  channel is smaller than for the  $\rho^0$  channel. Below we shall consider the  $\rho^0$  channel only, which is probably the most important.

The elastic  $\rho^0$ -production contribution (diagram (c) in Fig.5) to the semi-inclusive structure function (4,13) can be written formally as

$$\mathcal{F}_2^{\rho^0,el}(x, Q^2, z) = \frac{Q^2}{4\pi^2\alpha} \cdot \sigma_{\gamma^* N \rightarrow \rho^0 N}(W, Q^2) \cdot f_{\rho^0 \rightarrow \pi}(z), \quad (23)$$

The decay function  $f_{\rho^0 \rightarrow \pi}$  can be easily calculated (see Appendix B). For not too high energies, as for the HERMES experiment one may expect  $\sigma(\gamma^* p \rightarrow \rho^0 p) \neq \sigma(\gamma^* n \rightarrow \rho^0 n)$  which would modify the  $\bar{d} - \bar{u}$  asymmetry. At high energy the pomeron-exchange (two-gluon exchange) mechanism dominates and one may expect  $\sigma(\gamma^* p \rightarrow \rho^0 p) = \sigma(\gamma^* n \rightarrow \rho^0 n)$ . At low energy the exchange of subleading reggeons (quark exchange) could lead to  $\sigma(\gamma^* p \rightarrow \rho^0 p) \neq \sigma(\gamma^* n \rightarrow \rho^0 n)$  due to isovector contributions. In real photoproduction the isovector amplitude is known to be rather small [43]. In DIS the situation may be quite different. Assuming that the production is hard, i.e. of perturbative nature, the longitudinal  $\rho^0$  is predicted to be dominated by the quark exchange mechanism at low photon energies [44]. The HERMES  $\gamma^* p$  energy corresponds precisely to the maximum of the  $\rho_L^0$  production in the hard quark-exchange exclusive reaction  $\gamma^* p \rightarrow \rho_L^0 p$  [44, 45, 46, 47]. Although there are no experimental data in this region, the data from EMC [61], NMC [55] and E665 [62] collaborations in the close neighbourhood seem to be in rough agreement with the calculation for  $\sigma_L$  [44, 45]. Different quark distributions in the proton and neutron lead in this

approach to different  $\rho^0$  production cross sections for proton and neutron targets, which obviously leads to a different production rate of charged pions in reactions on the proton and neutron. This in turn modifies the right hand side of Eq.(8) and the subsequent conclusions on the  $\bar{d} - \bar{u}$  asymmetry.

One could also try to understand elastic meson production within the Regge phenomenology [49, 50]. It is not obvious a priori what is the kinematical range of applicability of either the quark exchange approach or Regge phenomenology. Below we shall investigate elastic  $\rho^0$  production on the proton and neutron using both these approaches:

- a) the Regge approach, and
- b) a QCD inspired quark-exchange model.

### 3.3.1 Regge approach

The cross section for neutral  $\rho$  meson electroproduction in the HERMES kinematics is not known experimentally. While for the proton target there are data in slightly different kinematical regions of  $x$  and  $Q^2$  [53], there is almost no data for the neutron target. Only in one work [54] was the  $\rho^0$  production studied simultaneously for the proton and deuteron data. The  $x$ - and  $Q^2$ -integrated result obtained there

$$\sigma_{incoher}(\gamma^* d \rightarrow \rho^0 pn) = ((0.7 - 0.8) \pm 0.2) \cdot \sigma(\gamma^* p \rightarrow \rho^0 p)$$

does not exclude the difference between the proton and neutron target. If the nuclear effects are completely ignored this leads to

$$\sigma(\gamma^* n \rightarrow \rho^0 n) = ((0.4 - 0.6) \pm 0.4) \cdot \sigma(\gamma^* p \rightarrow \rho^0 p).$$

However, in the present analysis we are interested in  $x$ - and  $Q^2$ -dependent cross sections. The only electroproduction data on the deuteron target with well defined kinematics were published in [55]. Such a limited set of the deuteron data does not allow us to determine the cross section on the neutron target for  $x$  and  $Q^2$  in the kinematical region we need. A possible way out would be to parametrize the proton data with a suitable, physically motivated parametrization in a possibly broad kinematical range (there are rich data around the kinematical region of the HERMES experiment, see Fig.9) and use theoretical arguments and/or experimental data for other reactions to determine the neutron cross sections.

In the present paper we shall parametrize the existing experimental data for exclusive  $\rho^0$  production by means of the following simple Regge-inspired reaction amplitude, similar to that in Ref.[49],

$$\begin{aligned}
A_{\lambda'_N \leftarrow \lambda_N}^{\lambda_V \leftarrow \lambda_{\gamma^*}}(\gamma^* N \rightarrow \rho^0 N; t) &= \left\{ i \cdot C_{\mathcal{P}}(t) \left( \frac{s}{s_0} \right)^{\epsilon_{\mathcal{P}}} + \left[ \frac{-1+i}{\sqrt{2}} \right] \cdot C_{IS}(t) \left( \frac{s}{s_0} \right)^{-1/2} \right. \\
&\pm \left. \left[ \frac{-1+i}{\sqrt{2}} \right] \cdot C_{IV}(t) \left( \frac{s}{s_0} \right)^{-1/2} \right\} \\
&\cdot \left[ \frac{m_\rho^2}{m_\rho^2 + Q^2} \right] \delta_{\lambda_{N'} \lambda_N} \delta_{\lambda_V \lambda_{\gamma^*}}
\end{aligned} \tag{24}$$

with “+” and “−” in front of the isovector ( $IV$ ) contribution for proton and neutron, respectively. The pomeron contribution is marked by  $\mathcal{P}$  and isoscalar reggeon contribution by  $IS$ . The following normalization is assumed:

$$\frac{d\sigma}{dt} = \frac{1}{(2s_N + 1)N_\lambda} \sum_{\substack{\lambda_N \lambda'_N \\ \lambda_{\gamma^*} \lambda_V}} \left| A_{\lambda'_N \leftarrow \lambda_N}^{\lambda_V \leftarrow \lambda_{\gamma^*}}(t) \right|^2, \tag{25}$$

where  $s_N$  is the spin of the nucleon and  $N_\lambda$  is the number of active helicity states of the virtual photon.

In the following we are interested in relatively low  $\gamma^* N$ -energies where in principle the pion-exchange mechanism could be important too. At low energies, just above resonances, the pion-exchange mechanism is known to be the dominant mechanism for photoproduction of  $\omega$  mesons [51, 52]. It can be shown that due to the helicity structure of its amplitude the pion-exchange contribution does not interfere with the diffractive contribution as far as the spin-averaged cross section is considered, that is the pion-exchange contribution can be added incoherently in the cross section. Because  $\Gamma_{\rho^0 \rightarrow \pi^0 + \gamma} \ll \Gamma_{\omega \rightarrow \pi^0 + \gamma}$  the relevant coupling constant  $f_{\gamma \rho^0 \pi}^2 = 96\pi \left( \frac{m_\rho^2}{m_\rho^2 - m_\pi^2} \right) \Gamma_{\rho\pi\gamma}$  is rather small. In order to estimate the corresponding cross section one has to make some plausible estimation for the vertex form factors. Assuming the form factors which lead to a good description of the  $\omega$ -photoproduction data, whilst neglecting other mechanisms, provides a reasonable upper estimate of the pion-exchange contribution for  $\rho^0$  production. The pion-exchange contribution estimated in this way can most probably be neglected in the kinematical region considered here. It is interesting to notice that unlike

for the neutral  $\rho$  meson production the pion-exchange contribution cannot be neglected for charged  $\rho$  meson production due to lack of the dominant isoscalar contributions. The discussion above further justifies the simple Ansatz used in (24).

In practical application we assume the same  $t$ -dependence of  $C_{\mathcal{P}}$ ,  $C_{IS}$  and  $C_{IV}$  and take  $\Lambda = m_\rho$ . The total  $\gamma^*N \rightarrow \rho^0N$  cross section can be obtained as the integral

$$\sigma(W, Q^2) = \int_{t_{min}(W, Q^2)}^{t_{max}(W, Q^2)} \frac{d\sigma}{dt}(t) dt. \quad (26)$$

There are many approximate or even incorrect formulas for the upper and lower integration limits in the literature. It is, however, essential to use correct formulas for small  $W$ .

The free parameters in Eq.(24) i.e.  $\epsilon_{\mathcal{P}}$ ,  $C_{\mathcal{P}}$  and  $C_{IS} + C_{IV}$ <sup>5</sup> have been fitted to the existing experimental data for the angle-integrated cross section for  $\rho^0$  production on hydrogen [53]. The slope parameter  $B$  in the exponential  $t$ -distribution was fixed at  $B = 6 \text{ GeV}^{-2}$  which is known experimentally.<sup>6</sup> In order to avoid poorly understood contributions of baryonic resonances we have limited our fit to  $W > 3 \text{ GeV}$ . The simple form of the amplitude above is obviously not adequate for large  $Q^2$  where genuine hard QCD processes take place. Consequently we have included in our fit only experimental data points with  $Q^2 < 10 \text{ GeV}^2$ . In Fig.9, together with all available  $\rho^0$  electroproduction data, we have shown these kinematical boundaries. The large filled circles denote the kinematical loci where the HERMES analysis of charged-pion semi-inclusive data was made. With the above cuts we get from the fit:  $C_{\mathcal{P}} = 1.57 \mu b^{1/2} \text{ GeV}^{-1}$ ,  $C_{IS} + C_{IV} = 6.33 \mu b^{1/2} \text{ GeV}^{-1}$  and  $\epsilon_{\mathcal{P}} = 0.102$ . The quality of the fit is shown in Fig.10. The corresponding  $\chi^2 = 2.34$ .

To separate the sum  $C_{IS} + C_{IV}$  into the isoscalar and isovector parts one needs more information. The size of the isovector  $a_2$ -exchange contribution was estimated long ago for total photoproduction cross section (see for instance [43]). It was found empirically that the total photoabsorption cross section on the proton and neutron can be parametrized at low energy as

$$\sigma_{tot} = \tilde{C}_{\mathcal{P}} + (\tilde{C}_f \pm \tilde{C}_{a_2}) E_{\gamma, LAB}^{-1/2}. \quad (27)$$

---

<sup>5</sup>It is impossible to separate the isoscalar and isovector reggeon contributions from the fit to the proton data only due to their identical energy dependence.

<sup>6</sup>The results are rather stable against a small variation of  $B$  in the range  $B = 6 \pm 2 \text{ GeV}^{-2}$ .

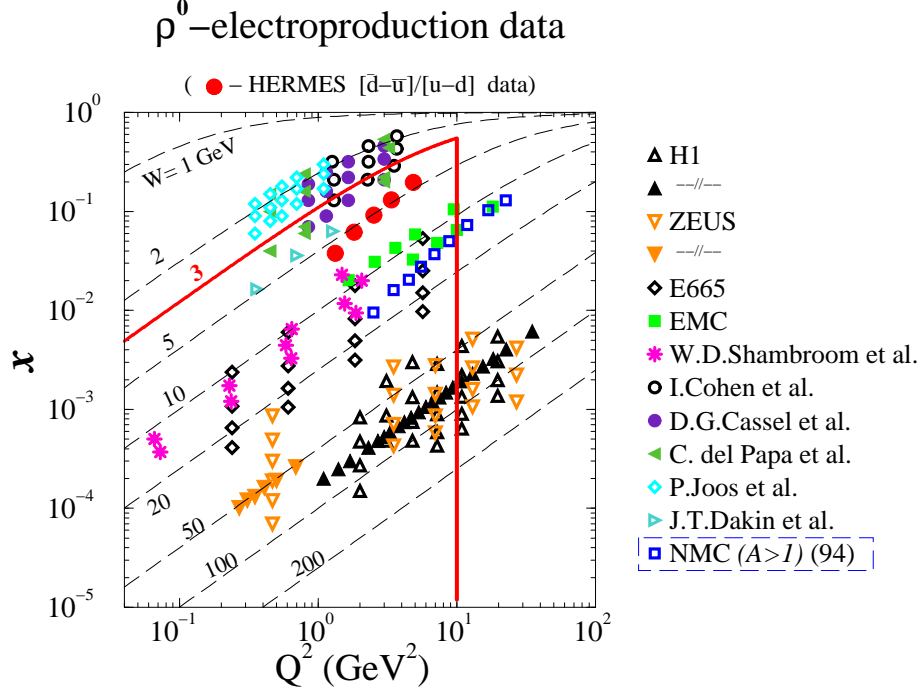


Figure 9: *Experimental data points for exclusive  $\rho^0$  production on the proton and deuteron (open squares). For illustration the HERMES kinematics is shown in addition by large solid circles. The thick solid lines show the limits for the Regge-inspired fit.*

In our parametrization of the  $\gamma^*p \rightarrow \rho^0p$  data the energy dependence of the pomeron- and reggeon-exchange contributions is slightly different (see Eq.(24)). Extending the validity of Regge phenomenology to both real and virtual photons we can write somewhat schematically the amplitude

$$A(\gamma^*N \rightarrow \gamma^*N) = \frac{m_V^4}{(m_V^2 + Q^2)^2} \left[ \left( \frac{1}{\gamma_{\rho^0}^2} + \frac{1}{\gamma_\omega^2} \right) P + \left( \frac{1}{\gamma_{\rho^0}^2} + \frac{1}{\gamma_\omega^2} \right) f \pm \frac{2}{\gamma_{\rho^0}\gamma_\omega} a_2 \right] \quad (28)$$

for Compton scattering,

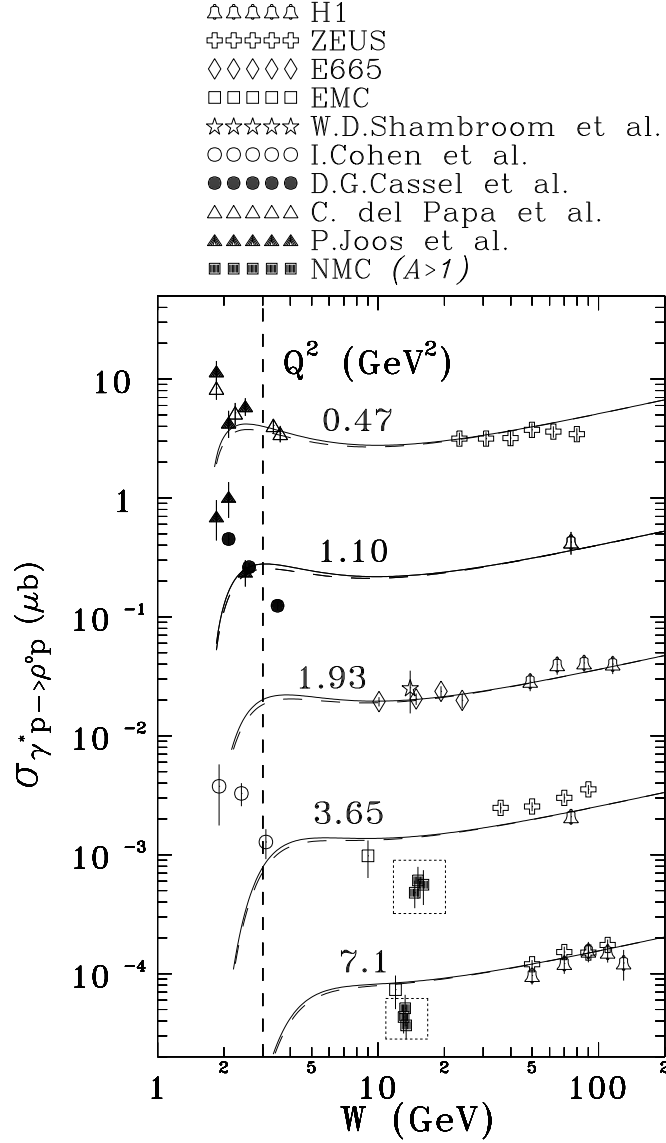


Figure 10: The cross section for  $\gamma^* p \rightarrow \rho^0 p$  as a function of center-of-mass energy for selected values of photon virtuality. The solid line is obtained from the VDM-Regge inspired fit. The dashed line shows the cross section on the neutron target. The solid squares represent the NMC nuclear data [55]. Please note that excepting  $Q^2 = 0.47$ , all other curves and experimental points are rescaled by 5,  $5^2$ ,  $5^3$  and  $5^4$ .



$$A(\gamma^*N \rightarrow \rho^0N) = \frac{m_V^2}{m_V^2 + Q^2} \left[ \frac{1}{\gamma_{\rho^0}} \mathcal{P} + \frac{1}{\gamma_{\rho^0}} f \pm \frac{1}{\gamma_\omega} a_2 \right] \quad (29)$$

for exclusive  $\rho^0$  photoproduction and

$$A(\gamma^*N \rightarrow \omega N) = \frac{m_V^2}{m_V^2 + Q^2} \left[ \frac{1}{\gamma_\omega} \mathcal{P} + \frac{1}{\gamma_\omega} f \pm \frac{1}{\gamma_{\rho^0}} a_2 \right] \quad (30)$$

for exclusive  $\omega$  photoproduction. We have used the values of  $\gamma_{\rho^0}$  and  $\gamma_\omega$  from [58] and put  $m_\rho = m_\omega \equiv m_V$ . Please note that  $\mathcal{P}$ ,  $f$  and  $a_2$  corresponding to the reggeon-exchange amplitudes on the hadronic level are the same in all these reactions. Different factors in front of these hadronic amplitudes give different strength of each contribution in different reactions. We have adjusted the relative strength of the  $a_2$ -contribution compared to the  $f$ -contribution in the Compton scattering amplitude (28) to reproduce the empirical low-energy parametrization (27) for  $\sigma_{tot}(\gamma p)$  and  $\sigma_{tot}(\gamma n)$ . In Fig.11 we compare  $\delta_{pn}^{Compton} = \frac{\sigma_{tot}(\gamma p) - \sigma_{tot}(\gamma n)}{\sigma_{tot}(\gamma p) + \sigma_{tot}(\gamma n)}$  given by the obtained parametrization with that from the empirical fit. Shown is the band due to the uncertainties of parameters from [43] and the best representation of the empirical formula by our Regge parametrization (24). Although we reproduce the empirical fit rather well, in our case there is a different relative strength of the  $f$  and  $a_2$  contributions to the Compton amplitude. This difference is caused by the energy dependence of the pomeron exchange as opposed to the constant assumed in the empirical fit [43].

Having fixed parameters in (28) we can calculate the corresponding proton-neutron asymmetry for  $\rho^0$  and  $\omega$  production:  $\delta_{pn}^{\rho^0}$ ,  $\delta_{pn}^\omega$ , which are also shown in Fig.11. We have shown in addition experimental results for  $\rho^0$  [56] and  $\omega$  [57] photoproduction which are consistent with our parametrization. While the asymmetry of the cross sections for the  $\rho^0$  production is similar to the Compton case, the asymmetry for the  $\omega$  production is considerably larger.<sup>7</sup> The latter may also be important in the context of  $\bar{d} - \bar{u}$  asymmetry. However, the absolute normalization of the corresponding cross section for the  $\gamma^*N \rightarrow \omega N$  reaction is not well known, at least in the region of the HERMES kinematics. It is expected to be considerably smaller than for the  $\rho^0$  production.

---

<sup>7</sup> We have neglected here the pion-exchange mechanism which would decrease  $\delta_{pn}^\omega$  at energies  $W < 5$  GeV.

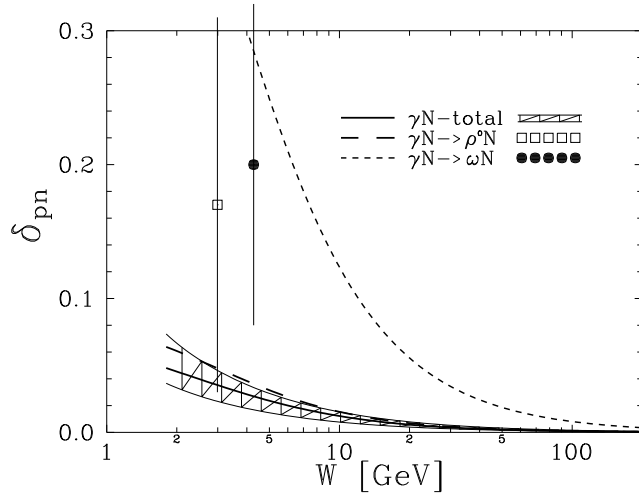


Figure 11: *The asymmetry  $\delta_{pn}$  as a function of center-of-mass energy. The thick solid line is obtained from the Regge parametrization adjusted to reproduce the empirical fit for total photoproduction (27) represented by the hatched band. The dashed and dotted lines correspond to a similar asymmetry for  $\rho^0$  and  $\omega$  production, respectively, and were obtained from our Regge parametrization. The experimental points are taken from [56] and [57].*

Although the difference of the cross sections for exclusive  $\rho^0$  production on the proton and neutron targets is small, the effect of this mechanism on the  $\bar{d} - \bar{u}$  asymmetry is not negligible at all. In Fig.12, we show the corresponding modification of the quantity  $\frac{\bar{d}-\bar{u}}{u-d}$  in the same way as before for the central VDM contribution. This modification may even be underestimated, as it is based on the Regge-inspired parametrization of the cross section for the  $\gamma^*n \rightarrow \rho^0n$  reaction which overestimates the  $\rho^0$  production on nuclei. This can be seen in Fig.10 where the NMC experimental points lie below the Regge-parametrization.

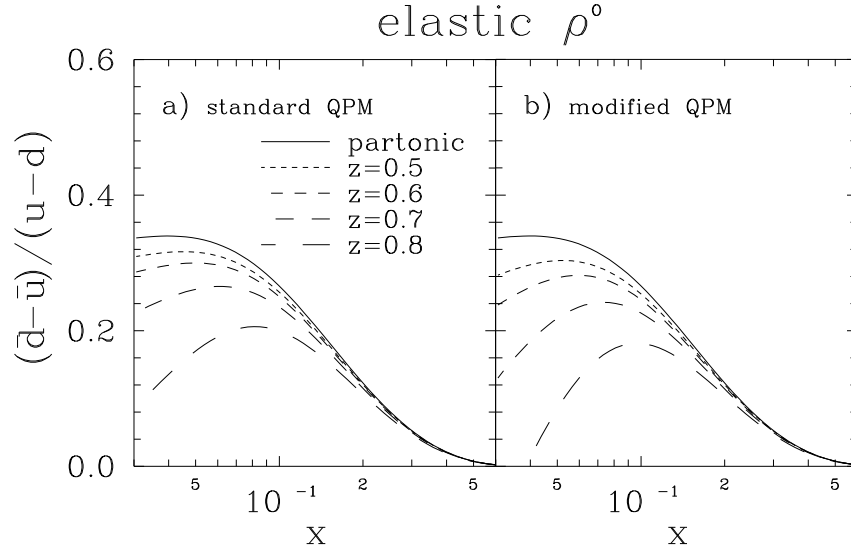


Figure 12: *The true (solid) and the modified by the exclusive  $\rho^0$  production  $(\bar{d}-\bar{u})/(u-d)$  as a function of Bjorken- $x$  for different  $z$  and typical HERMES  $W = 5$  GeV. As in the central VDM case, in panel (a)  $Q_0^2 = 0$  (standard partonic component) and in panel (b)  $Q_0^2 = 0.8$  GeV<sup>2</sup> (rescaled partonic component).*

### 3.3.2 QCD approach

For sufficiently large  $Q^2$ <sup>8</sup> the elastic vector meson production can be calculated perturbatively in the formalism of off-forward parton distributions (OFPD's) [44, 46]. It was argued that only the cross section for longitudinally polarized photons, where end-point contributions are suppressed, can be calculated reliably [59]. The cross section for the exclusive reaction  $\gamma_L^* + N \rightarrow V_L + N$  can be calculated in the standard way as

$$\frac{d\sigma_{LL}^{\gamma+N \rightarrow V+N}}{dt} = \frac{1}{16\pi s^2} \frac{1}{2} \sum_{\lambda_N \lambda'_N} |\mathcal{M}_{\lambda_N \lambda'_N}^{0,0}(t)|^2, \quad (31)$$

<sup>8</sup>It is not clear at present how large the virtuality should actually be for the applicability of this formalism.

where  $\lambda_N$  and  $\lambda'_N$  are helicities of the incoming and outgoing nucleons, respectively. The two zeros in the upper index row of the matrix element correspond to longitudinal photons and helicity 0 of the produced vector meson. The amplitude of the two-quark exchange mechanism for vector meson production was calculated for the first time in [44, 46]. The total longitudinal cross section can be obtained by integrating (31) over  $t$  in the kinematically allowed interval.

In the formalism first proposed by Ji [60], neglecting transverse momenta of quarks in the nucleons and in the vector meson, the leading order amplitude reads [45]

$$\mathcal{M}_{\lambda_N, \lambda'_N}^{0,0}(t) = -i \frac{4}{9} \frac{1}{Q} \int_0^1 dz \frac{\Phi_V(z)}{z(1-z)} \frac{1}{2} \int_{-1}^1 dx \left[ \frac{1}{x - \xi + i\epsilon} + \frac{1}{x + \xi - i\epsilon} \right] \cdot (4\pi\alpha_s) H_N^V(x, \xi, t) \bar{N}(p', \lambda'_N) \gamma \cdot n N(p, \lambda_N), \quad (32)$$

where  $\Phi_V(z)$  is the distribution amplitude and  $H_N^V(x, \xi, t)$  is a generalized function related to so-called skewed quark distributions in the nucleon. For the electroproduction of  $\rho^0$  mesons we are interested in here one gets

$$H_N^{\rho^0}(x, \xi, t) = \frac{1}{\sqrt{2}} \left[ \frac{2}{3} H^{u/N}(x, \xi, t) + \frac{1}{3} H^{d/N}(x, \xi, t) \right]. \quad (33)$$

The functions  $H^{u/N}(x, \xi, t) \equiv u_N(x, \xi, t)$  and  $H^{d/N}(x, \xi, t) \equiv d_N(x, \xi, t)$  are the non-diagonal, off-forward quark distributions. In this subsection we shall concentrate on the relative magnitude of the cross sections for  $\rho^0$  production off the neutron and proton. Therefore the approximation relying on the replacement of  $\xi \rightarrow x$  (i.e. using familiar diagonal quark distributions) seems sufficient for our present purpose. Consequently we shall take

$$\begin{aligned} H^{u/N}(x, \xi, t) &= u_N(x) \cdot D(t) \\ H^{d/N}(x, \xi, t) &= d_N(x) \cdot D(t) \end{aligned} \quad (34)$$

for  $x > 0$  and

$$\begin{aligned} H^{u/N}(x, \xi, t) &= -\bar{u}_N(x) \cdot D(t) \\ H^{d/N}(x, \xi, t) &= -\bar{d}_N(x) \cdot D(t) \end{aligned} \quad (35)$$

for  $x < 0$ . The above Ansatz assumes factorization of  $x$  and  $t$  dependences. Thus the whole  $t$ -dependence will be contained in one universal function  $D(t)$ , common for all flavours. We shall try exponential and dipole form

factors which provide a good representation of experimental data for exclusive  $\rho^0$  production. The factorized form has the advantage that the total longitudinal cross section can be obtained analytically.

In the present analysis we have neglected the tensor magnetic-type E-terms (see [45])<sup>9</sup> which may be expected to be important only at large  $t$  and lead therefore to a rather small contribution to the total cross section.

The integral in the amplitude given in (32) can be calculated in the standard way by splitting the integral into a real principle value and an imaginary  $\delta$ -function.

The cross section asymmetry defined as

$$\delta_{pn}^L \equiv \frac{\sigma_L^{\gamma^* p \rightarrow \rho^0 p} - \sigma_L^{\gamma^* n \rightarrow \rho^0 n}}{\sigma_L^{\gamma^* p \rightarrow \rho^0 p} + \sigma_L^{\gamma^* n \rightarrow \rho^0 n}} \quad (36)$$

calculated according to (31) and (32) is shown in Fig.13 as a function of photon-nucleon center-of-mass energy  $W$  for  $Q^2 = 4 \text{ GeV}^2$ , typical for the HERMES kinematics. As in previous calculations the quark distributions in Eqs.(34) and (35) were taken from [64]. If only valence quark distributions are taken into account there is a relatively large asymmetry between the scattering off the proton and neutron targets. The inclusion of sea quarks decreases the asymmetry, which vanishes completely at large energy (small  $x$  for a fixed  $Q^2$ ). At the energy of the HERMES experiment  $W \sim 5 \text{ GeV}$  there is about 10 percent asymmetry i.e. about a factor 2 more than in the Regge approach.

In Fig.14 we compare the asymmetry obtained within the Regge approach discussed in the previous section and within the perturbative formalism discussed here for fixed  $W$  (left panel) and fixed  $x$  (right panel) as a function of  $Q^2$ . There is a substantial difference between the Regge approach, where  $W$  is the variable relevant for the proton and neutron asymmetry, and the QCD approach, where it is rather Bjorken- $x$  which controls the asymmetry. In the Regge approach, if  $W$  is fixed the asymmetry is practically independent of  $Q^2$  and varies strongly for fixed Bjorken- $x$ . In contrast, in the perturbative approach for fixed Bjorken- $x$  the asymmetry only weakly depends on the photon virtuality, as can be seen from Fig.14b. If the center-of-mass energy is fixed instead, the  $Q^2$  dependence of the ratio is much stronger. As can be seen from Fig.14 the asymmetry between proton and neutron target becomes larger for larger photon virtuality.

---

<sup>9</sup>As far as we know these terms were never estimated in the literature.

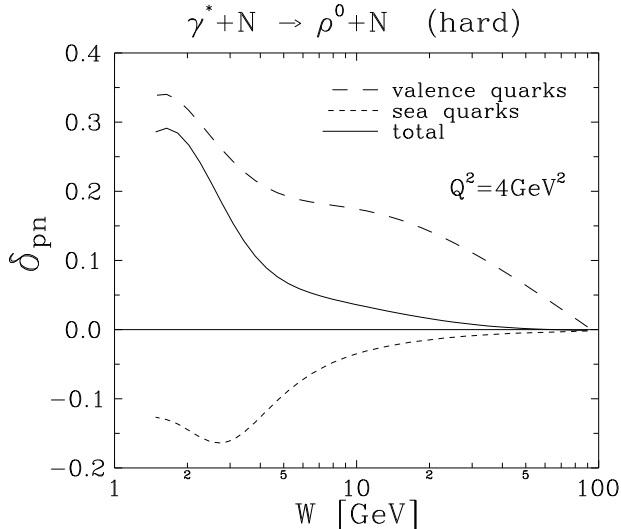


Figure 13:  $\delta_{pn}^L$  for quark-exchange mechanism as a function of center-of-mass energy. The solid line includes both valence and sea quarks. For completeness we show also the asymmetry for valence (dashed line) and sea (dotted) quarks exclusively.

We have calculated only longitudinal cross sections which dominate at large  $Q^2$ . At small  $Q^2$  the transverse cross section becomes equally important. Although it is not possible to make a rigorous calculation for the transverse cross sections, it is natural to expect  $\delta_{pn}^T$  and  $\delta_{pn}^L$  to be similar. Therefore we expect that the asymmetry for longitudinal cross sections should be a reasonable estimate of the asymmetry of the total (longitudinal+transverse) cross sections.

The description of the experimental data for exclusive  $\rho^0$  meson production by means of the hard mechanism (not discussed here) is not as good as by means of the Regge approach. The absolute normalization of the cross section depends on transverse momentum distributions of quarks in the nucleon and in the produced  $\rho$  meson [45] which are not fully understood at present. Therefore we shall not calculate here the corresponding modification of the measured  $(\bar{d} - \bar{u})/(u - d)$ . Such an analysis requires first of all a good description of the absolute value of the cross section. We expect, however, at least as big a modification as in the Regge case.

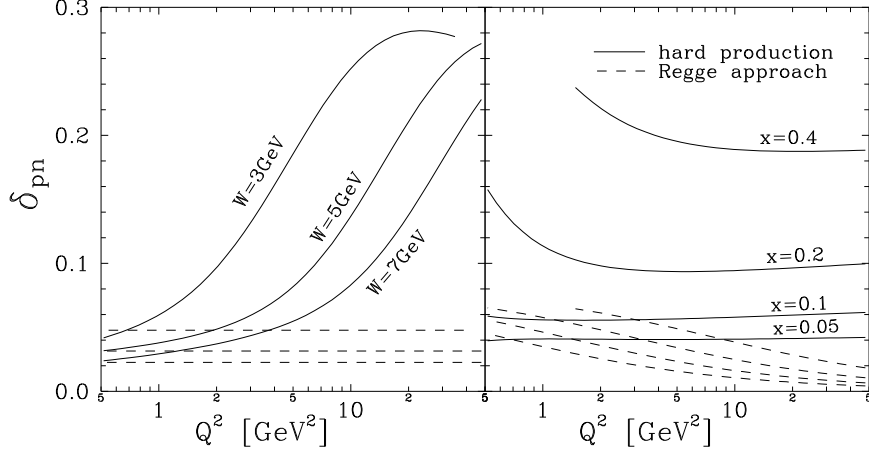


Figure 14:  $\delta_{pn}^L$  as a function of  $Q^2$  in the Regge (dashed) and QCD inspired (solid) approaches for: different fixed  $W = 3, 5, 7$  GeV (left panel) and different fixed Bjorken- $x = 0.05, 0.1, 0.2, 0.4$  (right panel).

### 3.3.3 Charged $\rho$ mesons

Above we have considered only neutral  $\rho$  mesons. Charged  $\rho$  mesons can also be a source of charged pions due to their decay mode  $\rho^\pm \rightarrow \pi^\pm \pi^0$ . Experimentally the cross section for exclusive charged  $\rho$  mesons is much less well known than that for the neutral  $\rho$  mesons. It can be estimated within the QCD formalism of the OFPDs approach as that sketched for neutral  $\rho$  mesons using symmetry relations for the matrix elements [47]. Because the cross section for exclusively produced charged mesons depends on quark distributions in the nucleon differently than in the QPM formula (4) the contribution of charged  $\rho$  mesons will certainly modify the  $\bar{d} - \bar{u}$  extracted by means of (8). Because the result depends on the magnitude of the charged-meson production which is rather difficult to predict in the QCD-type calculations (off-diagonal effects, the choice of the scale of the running coupling constant, inclusion of transverse momenta) we shall leave the problem for a separate more refined analysis.

## 4 Comments on nuclear effects in the deuteron

So far we have followed the HERMES collaboration and neglected all nuclear effects in the deuteron i.e. assumed that

$$\sigma(\gamma^*d \rightarrow \pi^\pm) = \sigma(\gamma^*p \rightarrow \pi^\pm) + \sigma(\gamma^*n \rightarrow \pi^\pm) . \quad (37)$$

The theory of nuclear effects in semi-inclusive processes is less developed than in the inclusive case. Let us consider a simple example of an  $x$ -independent relative nuclear effect of size  $\kappa$ , universal for produced  $\pi^+$  and  $\pi^-$ ,

$$\sigma(\gamma^*d \rightarrow \pi^\pm) = (1 - \kappa) (\sigma(\gamma^*p \rightarrow \pi^\pm) + \sigma(\gamma^*n \rightarrow \pi^\pm)) . \quad (38)$$

Then the semi-inclusive cross sections for pion production on the neutron extracted from the deuteron target data are

$$\begin{aligned} \sigma_{meas}(\gamma^*n \rightarrow \pi^\pm) &= \sigma(\gamma^*d \rightarrow \pi^\pm) - \sigma(\gamma^*p \rightarrow \pi^\pm) \\ &= (1 - \kappa)\sigma(\gamma^*n \rightarrow \pi^\pm) - \kappa\sigma(\gamma^*p \rightarrow \pi^\pm) \\ &= \sigma(\gamma^*n \rightarrow \pi^\pm) - \kappa (\sigma(\gamma^*p \rightarrow \pi^\pm) + \sigma(\gamma^*n \rightarrow \pi^\pm)) \end{aligned} \quad (39)$$

i.e. biased by the assumed nuclear effect  $\kappa$  in the deuteron.

Thus the differences  $\sigma(\gamma^*p \rightarrow \pi^\pm) - \sigma(\gamma^*n \rightarrow \pi^\pm)$  needed in Eq.(8) are replaced by

$$\begin{aligned} &\sigma(\gamma^*p \rightarrow \pi^\pm) - \sigma_{meas}(\gamma^*n \rightarrow \pi^\pm) = \\ &= (1 + \kappa)\sigma(\gamma^*p \rightarrow \pi^\pm) - (1 - \kappa)\sigma(\gamma^*n \rightarrow \pi^\pm) \\ &= \sigma(\gamma^*p \rightarrow \pi^\pm) - \sigma(\gamma^*n \rightarrow \pi^\pm) + \kappa (\sigma(\gamma^*p \rightarrow \pi^\pm) + \sigma(\gamma^*n \rightarrow \pi^\pm)) \end{aligned} \quad (40)$$

In Fig.15 we show the nuclear effects on  $\frac{\bar{d}-\bar{u}}{u-d}$  for  $\kappa = 0.02, 0.01, 0.0, -0.01, -0.02$ , i.e. in the range known from inclusive DIS. These effects are independent of  $z$  by assumption (38). Following the inclusive case, for small values of Bjorken  $x < 0.1$  a shadowing, i.e.  $\kappa > 0$  is expected which means that the asymmetry obtained when neglecting nuclear effects is underestimated (see Fig.15).

The shadowing leads to an effect opposite to that for the resolved photon component discussed earlier in this paper. For somewhat larger  $x$  an anti-shadowing due to excess pions is not excluded. For still larger  $x$  a nuclear binding and Fermi motion corrections come into play.

Summarizing, we have shown that even small nuclear effects, of the order of just a few percent, lead to considerable consequences for the  $\bar{d} - \bar{u}$



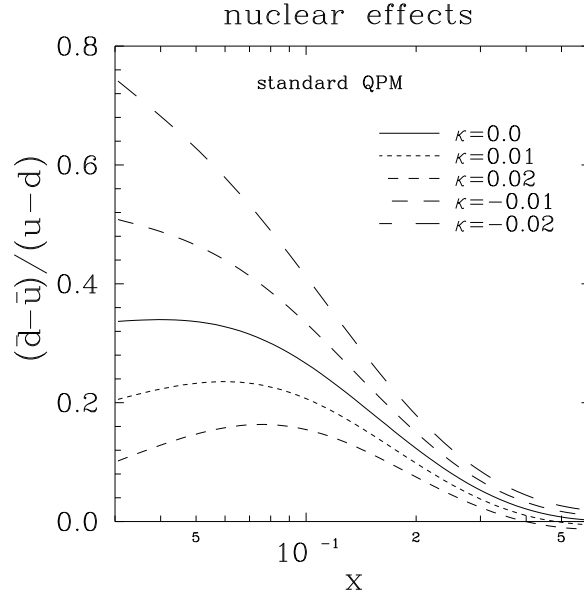


Figure 15: *The true (solid) and the modified by the nuclear effects  $(\bar{d} - \bar{u})/(u - d)$  as a function of Bjorken- $x$  for  $W = 5 \text{ GeV}$  and different values of  $\kappa$ .*

asymmetry. Nuclear effects are expected to be  $x$  and  $Q^2$  dependent. In the present analysis we have shown only a band of uncertainties due to nuclear effects. A more precise determination of the  $x$  or  $Q^2$  dependence requires a more microscopic calculation which goes beyond the scope of the present paper. This is, however, necessary if the  $\bar{d} - \bar{u}$  asymmetry is to be extracted from semi-inclusive data.

## 5 Consequences for the HERMES experiment

Having discussed each of the nonpartonic effects separately we will now attempt to combine them and try to understand their net effect on the measured  $\bar{d} - \bar{u}$  asymmetry, and the consequences of this for the HERMES data [7].

Before a numerical estimation of the total nonpartonic effect we would like to discuss briefly a subtle problem. At first sight it seems that fragmen-

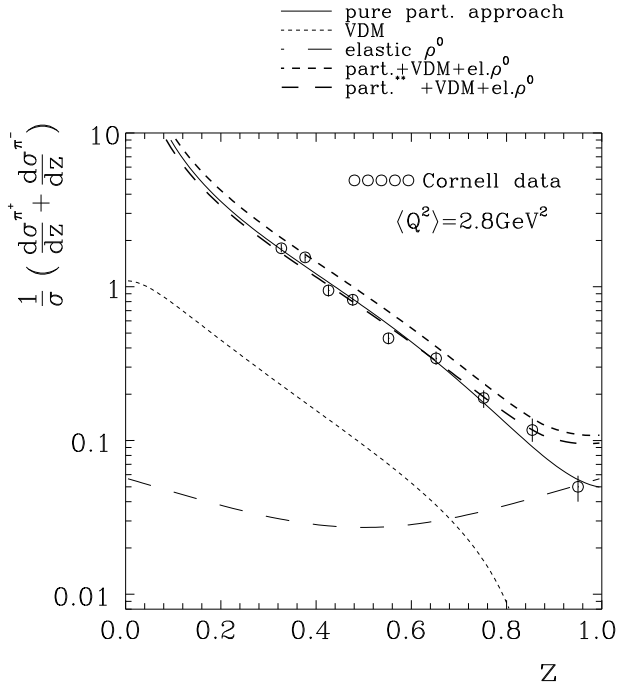


Figure 16: *Multiplicity distribution of the charged pions. Contributions of different mechanisms are shown separately. The total effect calculated in two different ways discussed in the text is also presented.*

tation functions fitted to experimental data effectively contain nonpartonic effects. This is most probably not true as nonpartonic components are higher-twist effects i.e. are strongly  $Q^2$ -dependent in contrast to the leading twist.

In section 2.3 we have selected the fragmentation functions which describe the pionic yields well. There is a danger a priori that explicit inclusion of the nonpartonic effects discussed in the present paper may worsen the description of pionic spectra. In Fig.16 we show the multiplicity of charged pions as a function of  $z$  for  $\langle Q^2 \rangle = 2.8 \text{ GeV}^2$  (compare with the left panel of Fig.2). Together with the corresponding Cornell data [18] we show the contributions due to different mechanisms separately. The contributions of nonpartonic mechanisms are considerably smaller than the main partonic contribution, however not negligible. If we add all of them together

we obtain the multiplicity (thick short-dashed line) over the experimental points. Another way to incorporate the partonic and nonpartonic components was proposed in Ref.[32] for the inclusive case. As can be seen from Fig.16, extension of this model to the semi-inclusive case, i.e. rescaling of the partonic component as in Eq.(13), (thick long-dashed line) provides a very good description of the experimental multiplicities. This approach treats all contributions explicitly, which seems more consistent than the approach mentioned above including them all effectively into fragmentation functions. It is also consistent with the inclusive structure function model [32].

In Fig.17 we show  $\frac{\bar{d}-\bar{u}}{u-d}$  as a function of  $z$  for different bins of Bjorken- $x$  (the averaged value of  $x$  is given in the figure). The data points are taken from [7]. The filled squares correspond to the data averaged over  $z$ . The QPM ( $z$ -independent) prediction with leading order quark distributions from [64] is shown for reference by the solid line. The results of the calculation including partonic, VDM and elastic  $\rho^0$  contributions are given by the dashed line (with the QPM contribution calculated in the standard way) and long-dashed line (with the QPM contribution modified as in Eq.(13)). As in the previous calculations the Field-Feynman fragmentation functions [21] were used here.

As can be seen from the figure there is a significant deviation of the “measured” asymmetry from the “real” one (the difference between the dashed and solid lines), especially for small values of Bjorken- $x$ . The effect is bigger for the “modified-QPM” approach i.e. for the more consistent one. The nuclear effects most probably will introduce further deviation which is, however, difficult to estimate numerically. A significant  $z$ -dependence casts doubts on the averaging in  $z$  at least in the whole range from 0 to 1. However, as seen from the figure the experimental statistics and the  $z$ -range of the HERMES experiment do not allow this dependence to be identified.

It is worth noting that the modification of the QPM result depends strongly on the fragmentation function used to calculate the ratio  $D_-/D_+$ . The Field-Feynman fragmentation functions used in the present analysis provide a good representation of the data from both EMC and HERMES (preliminary) (see Fig.4) i.e. are close to those used in extraction of the  $\bar{d}-\bar{u}$  asymmetry by the HERMES collaboration. One should also remember that the effect of elastic  $\rho^0$  production is model dependent, being generally larger in the hard production mechanism than in the Regge model. If we take our Regge result at face value we argue that the  $\bar{d}-\bar{u}$  asymmetry extracted by the HERMES collaboration is rather overestimated. In the present analysis

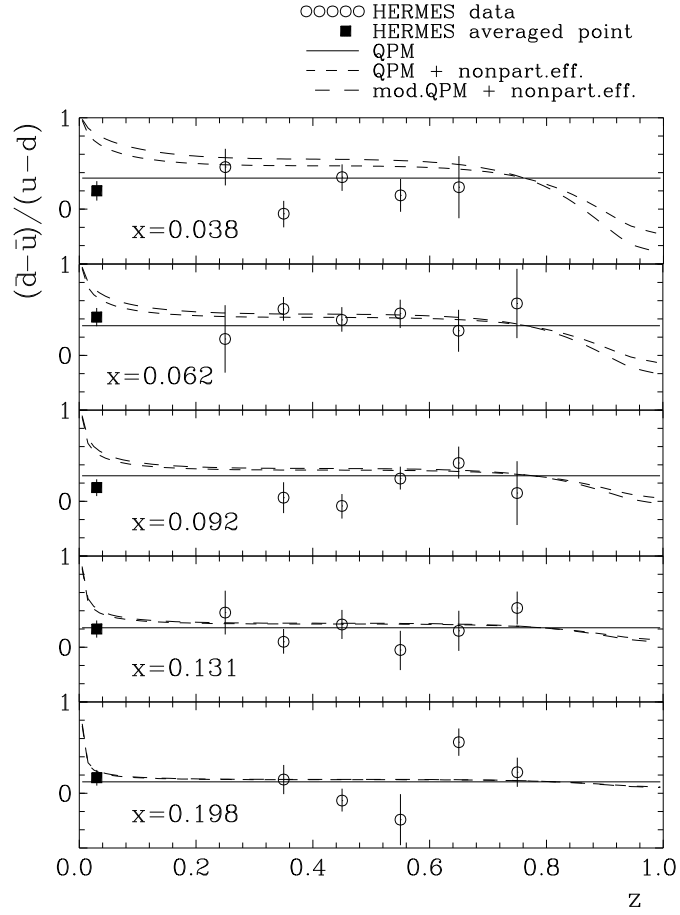


Figure 17:  $\frac{\bar{d}-\bar{u}}{u-d}$  as a function of  $z$  for different bins of  $x$ . The experimental data are from [7].

we do not attempt to correct the HERMES data for the effects discussed here. This requires a separate analysis including efficiencies of the HERMES apparatus as well as knowledge of the many cuts used in their analysis.

## 6 Conclusions

Extraction of parton densities is one of the main goals of high-energy physics. It was proposed some time ago how to use semi-inclusive production of charged pions to determine both unpolarized and polarized parton densities in the nucleons. Recently this idea was put into practice in both cases. Such analyses assume implicitly the validity of the quark-parton model. In a recent work of two of us [5] we have shown a breaking of the parton model in inclusive DIS at photon virtuality  $Q^2$  as large as 5-7 GeV<sup>2</sup> which is bigger than commonly perceived. The modern experiments analyzing semi-inclusive production of pions are performed in a similar range of  $Q^2$ . In general the situation in semi-inclusive reactions can be even more complex and subtle. In the present analysis we have made a first attempt to determine the nonleading mechanisms.

We have estimated a few effects beyond the quark-parton model which may influence the extraction of the  $\bar{d} - \bar{u}$  asymmetry from semi-inclusive production of pions in DIS.

Based on the analysis of hadronic data we have found that the interaction of the resolved hadron-like photon with the nucleon may lead to an artificial enhancement of the measured  $\bar{d} - \bar{u}$  asymmetry in the region of small  $x$ . Next, we have investigated the elastic production of  $\rho^0$  mesons by a virtual photon on the proton and neutron targets based on two different models. Unequal cross sections for proton and neutron targets also lead to an artificial modification of the  $\bar{d} - \bar{u}$  asymmetry extracted based on QPM formulae. The effect found is opposite to the effect due to the resolved photon component. These two effects cancel only in a narrow range of  $z$ . The net effect turned out to be  $z$ -dependent invalidating somewhat averaging in  $z$  as done recently in [7].

We suggest that instead of averaging over a broad range of  $z$  one could try to select the region of  $z$  ( $x$ - and  $Q^2$ -dependent) where the influence of nonpartonic effects is small. Unfortunately this can only be done at the expense of lowering the statistics considerably. An optimal choice of kinematical cuts in  $x$ ,  $Q^2$  and  $z$  requires a more detailed study. Clearly, increasing of  $Q^2$  looks helpful. This could be realized by HERMES or by an

as yet unproposed experiment for COMPASS at CERN.

Nuclear effects, even small ones, may also cloud the extraction of the true  $\bar{d} - \bar{u}$  asymmetry. To our knowledge there is no reliable estimate of such effects for semi-inclusive production of pions.

Although in the light of the present analysis the precise direct extraction of  $\bar{d} - \bar{u}$  is rather difficult, the semi-inclusive data can be used for tests of parton distributions, in particular the difference between  $\bar{d}$  and  $\bar{u}$ , provided nonpartonic and nuclear effects are understood and included in the analysis.

Finally we would like to point out that some of the effects discussed in the present paper may also influence the extraction of the polarized quark distributions from semi-inclusive production of pions in DIS. This will be a subject of a separate analysis.

## 7 Appendices

### A Parametrizing the $\pi p \rightarrow \pi X$ spectra in the pion hemisphere

The mechanism of inclusive pion production in hadronic reactions is in general not well understood. It is believed that rather soft processes dominate. Some progress was made recently in studying inclusive pion production in polarized scattering (for a review see [66]). In proton-proton scattering the large- $x_F$  region depends on the flavour structure of the outgoing pion. This part of the spectrum was explained e.g. in the recombination model [67], fusion model [68] and recently in the meson cloud model [69, 70, 71]. The central (mid-rapidity) part of the spectrum seems to be flavour independent [68].

The inclusive spectra of pions in pion-nucleon scattering are, in general, even less well understood. For beam-like pions the large- $x_F$  part of the spectra seems to be dominated by diffractive processes due to pomeron or reggeon ( $f$  or  $\rho^0$ ) exchanges. For both beam-like and beam-unlike spectra one may expect a nonnegligible contribution from the decay of  $\rho$  mesons produced in peripheral processes  $\pi + p \rightarrow \rho + X \rightarrow (\pi + \pi) + X$ , dominated by pion exchange.

The most complete experimental data for the  $\pi^\pm p \rightarrow \pi^\pm X$  reactions were collected by the ABBCCHW collaboration at the CERN hydrogen bubble chamber [36]. A detailed analysis of the  $\pi^+ p \rightarrow \pi^\pm X$  and  $\pi^- p \rightarrow \pi^\pm X$  two-dimensional spectra [36] combined with a general understanding of the

reaction mechanism have shown that the spectra of all 4 reactions ( $4 \times 10 = 40$  spectra) can be represented by the following six-component Ansatz:

$$\begin{aligned}
\frac{d\sigma^{i \rightarrow j}}{dx_F dp_\perp^2} &= C_{soft} \left(1 - \frac{\eta}{\eta_{max}}\right)^{p_{soft}} \frac{\partial \eta}{\partial x_F} \cdot e^{-B_{soft} p_\perp^2} \\
&+ C_{hard}^{ij} \cdot f_{hard}(x_F) \cdot e^{-B_{hard} p_\perp^2} \\
&+ C_{cen}^{ij} \cdot e^{\frac{x_F^2}{2\sigma_{cen}^2}} \cdot e^{-B_{cen} p_\perp^2} \\
&+ C_P \cdot x_F (1 - x_F)^{\alpha_P} \cdot e^{-B_P p_\perp^2} \\
&+ C_R \cdot x_F (1 - x_F)^{\alpha_R} \cdot e^{-B_R p_\perp^2} \\
&+ C_\rho^{ij} \cdot f_\rho(x_F) \cdot e^{-B_\rho p_\perp^2}, \tag{41}
\end{aligned}$$

where the maximal rapidity  $\eta_{max} = \eta_{max}(p_\perp^2)$ .

Each of the components above corresponds to a distinct physical mechanism, the first three to central processes and the last three to peripheral processes. By analogy with  $pp$  collisions [68] we have assumed one universal (flavour independent) soft component and allow for different normalization of flavour dependent components, called here hard due to their transverse momentum dependence. We have found  $B_{soft} = 8.5 \text{ GeV}^{-2}$  and  $B_{hard} = 3.0 \text{ GeV}^{-2}$ , consistent with characteristic slopes of soft and hard processes. The parametrization of the soft component gives a multiplicity rising with the energy in the entrance channel. Some models in the literature predict a growth of the flavour asymmetric part of the inclusive cross section with energy, some predict that it should stay almost constant. Therefore in the present paper we have tried different functional forms for the phenomenological flavour dependent part called here the hard component:

$$f_{hard}(x_F) = \begin{cases} (1 - x_F^2)^{p_{hard}}, \\ (1 - \frac{\eta}{\eta_{max}})^{p_{hard}} \frac{\partial \eta}{\partial x_F}. \end{cases} \tag{42}$$

In the present schematic parametrization we have taken  $\alpha_P = 1$  and  $\alpha_R = 0.5$ , i.e. we have neglected  $t$ -dependence of the Regge trajectories. By comparison with the experimental data we found  $B = 5.0 \text{ GeV}^{-2}$ . The extra factor  $x_F$  in front of the diffractive components was added to extrapolate smoothly down to  $x_F = 0$ . We have found that peripheral production of  $\rho$  mesons due to pion exchange and their subsequent decay constitutes a nonnegligible source of charged pions. Inspired by the pion exchange model and consistently with the data we have fixed the relations between

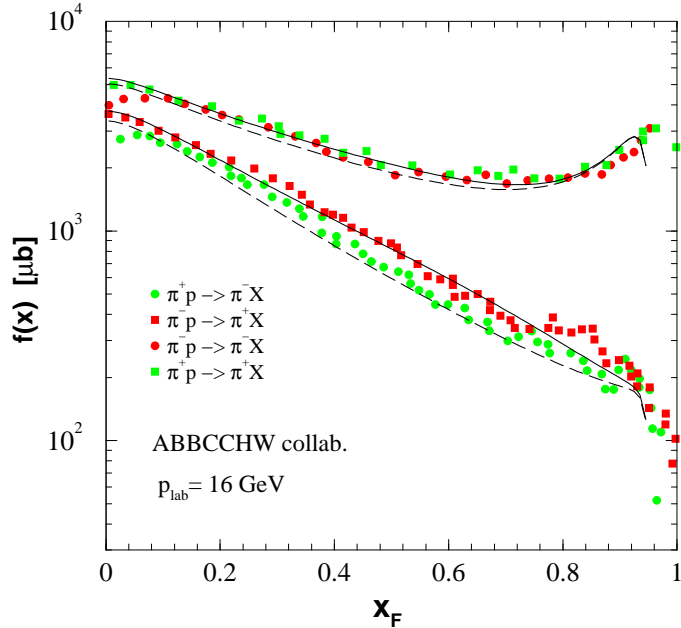


Figure 18: *An example of the quality of the parametrization (41). The experimental data points were scanned from Fig.1 in [36].*

normalization constants for such different processes

$$C_{\rho}^{++} \approx C_{\rho}^{--} \approx 2C_{\rho}^{-+} \approx 2C_{\rho}^{+-}.$$

The functional form of  $f_{\rho}(x_F)$  has been taken from a schematic model calculation and one normalization parameter  $C_{\rho}$  was fitted to the two-dimensional spectra, which is possible because this mechanism dominates the beam-unlike spectra at  $x_F > 0.7$ .

The nature of the phenomenological very central, very soft ( $B_{cen} = 20$ - $30 \text{ GeV}^{-2}$ ) component is not clear. It was introduced only to describe the data. It is most probably associated with pions from the decay of non-peripheral  $\rho$  mesons. We have found empirically approximately the same relation for normalization constants  $C_{cen}^{ij}$  as for  $C_{\rho}^{ij}$ .

In Fig.18 we present the quality of our fit for transverse momentum integrated  $x_F$ -distributions for all four reactions  $\pi^{\pm}p \rightarrow \pi^{\pm}X$ . The results



are shown in terms of the invariant single particle structure function [36]

$$f(x_F) = \frac{1}{\pi} \int_0^\infty \frac{E^*}{p_{max}^*} \frac{d^3\sigma}{dx_F dp_\perp^2} dp_\perp^2. \quad (43)$$

## B $\rho$ meson decay functions

In order to calculate the decay function in the most general case one needs to include off-diagonal elements of the density matrix [72]. In the present paper we shall neglect the probably small off-diagonal effects. Then the decay function  $f(z)$  depends on the helicity of the parent  $\rho^0$  meson. In the general case of broad resonance it can be calculated as:

$$f_\lambda(z_{\pi/\rho}) = \int dm_\rho \rho(m_\rho) \int d\Omega [f_\lambda(\theta, \phi) \delta(z(\theta, \phi) - z_{\pi/\rho})], \quad (44)$$

where  $f_\lambda(\theta, \phi) = |Y_{1\lambda}(\theta, \phi)|^2$  is the angular distribution of pions in the rest frame of  $\rho$  and  $\rho(m_\rho)$  is the spectral density. The momentum fraction of a pion with respect to the parent  $\rho$  meson is:

$$z_{\pi/\rho} = \frac{p_z^\pi(m_\rho) + p_0^\pi(m_\rho)}{m_\rho} \approx \frac{1}{2}(1 + \cos \theta), \quad (45)$$

which is independent of  $m_\rho$ . The last relation is due to the smallness of the pion mass and must be corrected in the case of soft pions. In the approximation used in the present paper the two integrals in (44) factorize and one easily gets

$$f_\lambda(z) \approx \begin{cases} 6z(1-z) & \text{for } \lambda = \pm 1, \\ 3(2z-1)^2 & \text{for } \lambda = 0, \end{cases} \quad (46)$$

where above  $z$  is used instead of  $z_{\pi/\rho}$  for brevity.

For the exclusive reaction  $\gamma^* N \rightarrow \rho^0 N$  at high energy one has  $z \equiv z_{\pi/\gamma} \approx z_{\pi/\rho}$ . For semi-inclusive production through quark hadronization the decay function (44) must be convoluted with the fragmentation function into the  $\rho$  meson  $D_{q \rightarrow \rho}$ . Below we shall consider these two distinct cases of  $\rho$  meson production.

In inclusive unpolarized production of  $\rho$  mesons one may expect approximately an equal population of different helicities due to the complexity

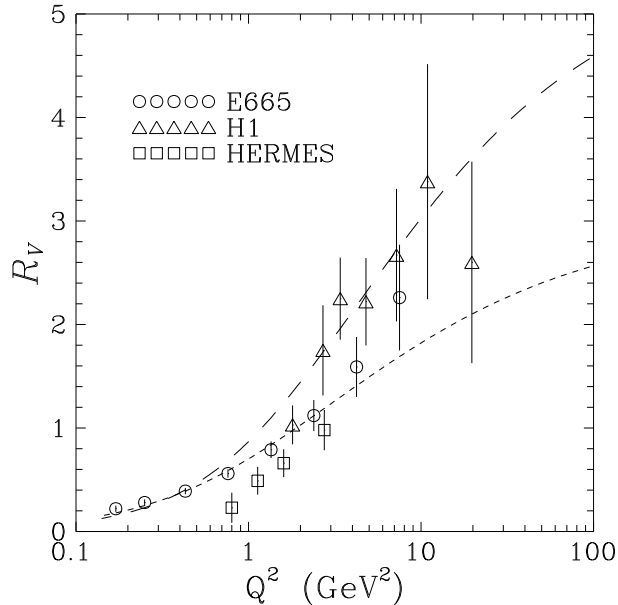


Figure 19:  $R_V$  as a function of the photon virtuality. The experimental data are from [75, 76] while the parametrizations are from [74]. The long-dashed and the short-dashed lines correspond to the 2- and 4-parameter fits, respectively.

of the poorly understood hadronization process. Then the effective decay function, which is averaged over  $\rho$  meson helicities, becomes

$$f(z) \approx \frac{1}{3}[2f_1(z) + f_0(z)] \approx \text{const} . \quad (47)$$

In the most general case of exclusive  $\rho$  meson electroproduction the angular distribution of pions can be obtained according to the formalism of Schilling and Wolf [73]. For sufficiently large energy, where  $s$ -channel helicity conservation takes place, averaging over azimuthal angle, the effective decay function can be approximated as

$$f(z) \approx \frac{f_1(z) + \epsilon R_V(Q^2, W) f_0(z)}{1 + \epsilon R_V(Q^2, W)} , \quad (48)$$

where the polarization parameter  $\epsilon = \epsilon(s_{eN}^{1/2}, W, Q^2) = \frac{1-y}{1-y+y^2/2}$  measures

the degree of longitudinal polarization of virtual photons. The effective decay function (48) depends on  $Q^2$  due to the empirically known strong  $Q^2$ -dependence of  $R_V = \sigma(\gamma_L N \rightarrow \rho^0 N) / \sigma(\gamma_T N \rightarrow \rho^0 N)$ . Some smooth dependence of  $R_V$  on  $W$  or  $x$  is not excluded a priori. We shall take the model parametrization of  $R_V(Q^2, W)$  from [74] (the 4-parameter fit) which, as shown in Fig.19, adequately describes the experimental data from [75, 76]. We show there also recent HERMES experimental data [77] which lie below the parametrization. Since the HERMES data were taken on the  $^3\text{He}$  target this may be partially caused by poorly understood nuclear effects.

**Acknowledgments** We are indebted to the members of the HERMES collaboration for discussions of their recent results and details of their apparatus and analysis, in particular Alexander Borissov, Naomi Makins, Pasquale di Nezza, Valeria Muciffora and Manuella Vincter. We are also indebted to Kolya Nikolaev for an informative discussion and pointing us to some interesting references, Lech Mankiewicz for a critical remark, Andrzej Sandacz for pointing out some experimental data, unknown to us, for elastic  $\rho^0$  production and Marc Vanderhaeghen for a discussion of the details of their QCD-inspired calculation of the quark-exchange mechanism. Finally we are indebted to Martin Kimber for a careful reading of the manuscript. This work was partially supported by the German-Polish DLR exchange program, grant number POL-028-98.

## References

- [1] P. Amaudruz et al. (NMC), Phys. Rev. Lett. **66** (1991) 2712.
- [2] J. Speth and A.W. Thomas, Adv. Nucl. Phys. **24** (1998) 83;  
S. Kumano, Phys. Rep. **303** (1998) 183.
- [3] A. Baldit et al. (NA51 collaboration), Phys. Lett. **B332** (1994) 244.
- [4] E.A. Hawker et al. (E866/NuSea collaboration), Phys. Rev. Lett. **80** (1998) 3715.
- [5] A. Szczurek and V. Uleshchenko, hep-ph/9911467, Phys. Lett. **B475** (2000) 120.
- [6] J. Levelt, P.J. Mulders and A.W. Schreiber, Phys. Lett. **B263** (1991) 498.

- [7] K. Ackerstaff et al. (HERMES collaboration), Phys. Rev. Lett. **81** (1998) 5519.
- [8] P.L. Anthony et al. (E155 collaboration), Phys. Lett. **B458** (1999) 536.
- [9] A. Afanasev, C.E. Carlson and Ch. Wahlquist, hep-ph/9903493.
- [10] J. Levelt and P.J. Mulders, Phys. Rev. **D49** (1994) 96.
- [11] R.P. Feynman, Photon-Hadron Interactions, Benjamin, 1972.
- [12] M. Adamus et al. (NA22 collaboration), Phys. Lett. **B183** (1987) 425;  
M. Aguilar-Benitez et al. (LEBC-EHS collaboration), Z. Phys. **C44** (1989) 531.
- [13] E. Kogan et al., Nucl. Phys. **B122** (1977) 383;  
M. Atkinson et al. (Omega Photon collaboration), Nucl. Phys. **B245** (1984) 189;  
R.J. Apsimon et al. (Omega Photon collaboration), Z. Phys. **53** (1992) 581.
- [14] I. Cohen et al., Phys. Rev. **D25** (1982) 634.
- [15] P. Chiappetta, M. Greco, J. Ph. Guillet, S. Rolli and M. Werlen, Nucl. Phys. **B412** (1994) 3.
- [16] J. Binnewies, B.A. Kniehl and G. Kramer, Z. Phys. **C65** (1995) 471.
- [17] J. Binnewies, B.A. Kniehl and G. Kramer, Phys. Rev. **D52** (1995) 4947.
- [18] G. Drews et al., Phys. Rev. Lett. **41** (1978) 1433.
- [19] J.J. Aubert et al. (EMC), Phys. Lett. **B160** (1985) 417.
- [20] C.E. Carlson and A.B. Wakely, Phys. Rev. **D48** (1993) 2000.
- [21] R.D. Field and R.P. Feynman, Phys. Rev. **D9** (1977) 2590.
- [22] R.D. Field and R.P. Feynman, Nucl. Phys. **B136** (1978) 1.
- [23] R. Baier and K. Fey, Z. Phys. **C2** (1979) 339.
- [24] G. Altarelli, R.K. Ellis, G. Martinelli and S.-Y. Pi, Nucl. Phys. **B160** (1979) 301.

- [25] P. Abreu et al. (DELPHI collaboration), Phys. Lett. **406** (1997) 271.
- [26] S. Behrends et al. (CLEO collaboration), Phys. Rev. **D31** (1985) 2161.
- [27] H. Albrecht et al. (ARGUS collaboration), Z. Phys. **C61** (1994) 1.
- [28] I. Cohen et al., Phys. Rev. **D25** (1982) 634.
- [29] H. Albrecht et al. (ARGUS collaboration), Z. Phys. **C44** (1989) 547.
- [30] M.T. Ronan et al. (SPEAR collaboration), Phys. Rev. Lett. **44** (1980) 367.
- [31] J. Kwieciński and B. Badełek, Z. Phys. **C43** (1989) 251;  
B. Badełek and J. Kwieciński, Phys. Lett. B295 (1992) 263.
- [32] A. Szczurek and V. Uleshchenko, hep-ph/9904288, Eur. Phys. J. **C12** (2000) 663.
- [33] M. Arneodo et al. (EM collaboration), Nucl. Phys. **B321** (1989) 541.
- [34] Ph. Geiger, PhD thesis, Ruprecht-Karl-Universität, Heidelberg 1998.
- [35] P. di Nezza, PhD thesis, Perugia University, Perugia 1998.
- [36] P. Bosetti et al. (ABBCCHW collaboration), Nucl. Phys. **B54** (1973) 141.
- [37] A. Szczurek, H. Holtmann and J. Speth, Nucl. Phys. **A605** (1996) 496.
- [38] Review of Particle Physics, Particle Data Group, Eur. Phys. J. **C3** (1998) 209.
- [39] K. C. Moffeit et al., Phys. Rev. **D5** (1972) 1603.
- [40] K. Nakayama, A. Szczurek, Ch. Hanhart, J. Heidenbaur and J. Speth, Phys. Rev. **C57** (1998) 1580.
- [41] A. Donnachie and P.V. Landshoff, Phys. Lett. **B296** (1992) 227.
- [42] M. Fontannaz, A. Mantrach, D. Schiff and B. Pire, Z. Phys. **C6** (1980) 241.
- [43] D.W.G.S. Leith in Electromagnetic Interactions of Hadrons, edited by A. Donnachie and G. Shaw, Plenum Press, New York 1978.

- [44] M. Vanderhaeghen, P.A.M. Guichon and M. Guidal, Phys. Rev. Lett. **80** (1998) 5064.
- [45] M. Vanderhaeghen, P.A.M. Guichon and M. Guidal, hep-ph/9905372, Phys. Rev. **D60** (1999) 094017.
- [46] L. Mankiewicz, G. Piller and T. Weigl, Eur. Phys. J. **C5** (1998) 119.
- [47] L. Mankiewicz, G. Piller and T. Weigl, Phys. Rev. **D59** (1999) 017501.
- [48] L. Mankiewicz, G. Piller and A. Radyushkin, hep-ph/9812467.
- [49] A. Donnachie and P.V. Landshoff, Phys. Lett. **B348** (1995) 213.
- [50] L.P.A. Haakman, A. Kaidalov and J.H. Koch, Phys. Lett. **B365** (1996) 411.
- [51] P. Joos et al., Nucl. Phys. **B122** (1977) 365.
- [52] A.I. Titov and Y. Oh, Phys. Lett. **B422** (1998) 33.
- [53] J.T. Dakin et al., Phys. Rev. **D8** (1973) 687;  
P. Joos et al., Nucl. Phys. **B113** (1976) 53;  
C. del Papa et al., Phys. Rev. **D19** (1979) 1303;  
D.G. Cassel et al., Phys. Rev. **D24** (1981) 2787;  
I. Cohen et al., Phys. Rev. **D25** (1982) 634;  
W.D. Shambroom et al., Phys. Rev. **D26** (1982) 1;  
J.J. Aubert et al. (EM collaboration), Phys. Lett. **B161** (1985) 203;  
M.R. Adams et al. (E665 collaboration), Z. Phys. **C74** (1997) 237;  
J. Breitweg et al. (ZEUS collaboration), Eur. Phys. Jour. **C6** (1999) 603;  
C. Adloff et al. (H1 collaboration), hep-ex/9902019, submitted to Eur. Phys. J. **C**.
- [54] M.R. Adams et al. (E665 collaboration), Phys. Rev. Lett. **74** (1995) 1525.
- [55] M. Arneodo et al. (NMC), Nucl. Phys. **B429** (1994) 503.
- [56] Y. Eisenberg et al., Nucl. Phys. **B42** (1972) 349.
- [57] J. Abramson et al., Phys. Rev. Lett. **36** (1976) 1428.

- [58] B.L. Ioffe, V.A. Khoze, L.N. Lipatov, *Hard Processes; Phenomenology, Quark-Parton Model*, North-Holland, Amsterdam 1984.
- [59] J.C. Collins, L. Frankfurt and M. Strikman, *Phys. Rev.* **D56** (1997) 2982.
- [60] X. Ji, *Phys. Rev.* **D55** (1997) 7114.
- [61] J.J. Aubert et al. (EM collaboration), *Z. Phys.* **C39** (1988) 169.
- [62] M.R. Adams et al. (E665 collaboration), *Z. Phys.* **C74** (1997) 237.
- [63] M. Arneodo et al. (NM collaboration), *Phys. Rev.* **D50** (1994) R1.
- [64] M. Glück, E. Reya and A. Vogt, *Z. Phys.* **C67** (1995) 433.
- [65] A.D. Martin, R.G. Roberts, W.J. Sirling and R.S. Thorne, hep-ph/9803445, *Eur. Phys. Jour.* **C4** (1998) 463.
- [66] Liang Zuo-Tang and C. Boros, hep-ph/0001330.
- [67] K.P. Das and R.C. Hwa, *Phys. Lett.* **B68** (1977) 459.
- [68] Liang Zuo-tang and Meng Ta-chung, *Phys. Rev.* **D49** (1994) 3759.
- [69] N.N. Nikolaev, W. Schäfer, A. Szczurek and J. Speth, *Phys. Rev.* **D60** (1999) 014004.
- [70] F. Carvalho, F.O. Duraes, F.S. Navarra and M. Nielsen, *Phys. Rev.* **D60** (1999) 094015.
- [71] C. Boros, *Phys. Rev.* **D59** (1999) 051501.
- [72] M. Anselmino, M. Bertini, F. Murgia and B. Pire, *Phys. Lett.* **B438** (1998) 347.
- [73] K. Schilling and G. Wolf, *Nucl. Phys.* **B61** (1973) 381.
- [74] D. Schildknecht, G.A. Schuler and B. Surrow, *Phys. Lett.* **B449** (1999) 328.
- [75] M.R. Adams et al. (E665 collaboration), *Z. Phys.* **C74** (1997) 237.
- [76] S. Aid et al. (H1 collaboration), *Nucl. Phys.* **B468** (1996) 3.
- [77] R. Ackerstaff et al. (HERMES collaboration), hep-ex/0002016.